Author:
Moller-Clarke, Jaydon C

Title:
Modulation of L-lactate release by astrocytic GABAB receptors and cyclic AMP signalling in vitro

Modulation of L-lactate release by astrocytic $GABA_B$ receptors and cyclic AMP signalling in vitro

Jaydon Moller-Clarke

A dissertation submitted to the University of Bristol in accordance with the requirements for award of the degree of MSci by Research in the Faculty of Life Sciences

School of Physiology, Pharmacology and Neuroscience
07/21
Word Count: 10739

Abstract:

Astrocytes are crucial for the maintenance of the excitation/inhibition balance of neural circuits and therefore must sense and respond to local neuronal activity. Their regulation of glutamatergic transmission is currently better understood than that of GABAergic. While $GABA_B$ receptor activation is generally associated with $G_{i/o}$ protein signalling, previous work in astrocytes suggested an additional IP_3-dependent pathway leading to intracellular Ca^{2+} oscillations. In this study, we set out to investigate whether the $GABA_B$ receptor agonist baclofen modulates production and release of the gliotransmitter L-lactate (LL) in dissociated primary astrocyte cultures. Specifically, we focused on the cyclic AMP (cAMP) dependent pathway which has been linked glycogenolysis. We used the FRET-based nanosensor Laconic to monitor intracellular LL dynamics and a fluorimetric LL assay (EnzyFluo) to measure LL release. We found that baclofen (10μM-100μM) inhibited production of LL (88±24.9% ; n=15) in unstimulated astrocytes, and that LL production and release under these conditions was partially glycogen-dependent. However, presumably since basal constitutive LL release was low, an inhibitory effect of baclofen on release was not detectable. Activation of adenylyl cyclase by NKH 477 (6-[3-(dimethylamino)propionyl]-forskolin; 0.3μM-30μM) resulted in LL mobilisation in a concentration dependent manner. Interestingly, intracellular LL increase peaked at 3μM NKH, but LL release from the cells peaked at 10μM NKH, suggesting potentially differential effects of cAMP signalling on LL production and release mechanisms. The cAMP driven LL production was inhibited by activation of $GABA_B$ receptors with baclofen (100μM), or by blocking glycogenolysis with DAB (1,4-Dideoxy-1,4-imino-D-arabinitol; 500μM), or PKA activity with H89 (10μM). Whilst the effect of baclofen on the NKH-stimulated rise of cAMP signalling was abolished by inhibition of $G_{i/o}$ signalling with Pertussis toxin (PTX), PTX application did not abolish the effect of baclofen on the NKH-stimulated rise of intracellular LL. Our preliminary observations also suggest that inhibition of $G_{i/o}$ signalling with PTX may increase LL release. Further work is needed to evaluate the effects of any cross-talk between cAMP and Ca^{2+} signalling pathways on LL release.

Author's declaration

I declare that the work in this dissertation was carried out in accordance with the requirements of the University's *Regulations and Code of Practice for Research Degree Programmes* and that it has not been submitted for any other academic award. Except where indicated by specific reference in the text, the work is the candidate's own work. Work done in collaboration with, or with the assistance of, others, is indicated as such. Any views expressed in the dissertation are those of the author.

SIGNED: JAYDON MOLLER-CLARKE DATE:05/08/21

Table of Contents

Abbreviations:

AC: Adenylyl Cyclase

ANLS: Astrocyte-Neuron Lactate Shuttle

AR-C: **6**-[(3,5-Dimethyl-1H-pyrazol-4-yl)methyl]-5-[[(4S)-4-hydroxy-2-isoxazolidinyl]carbonyl]-3-methyl-1-(2-methylpropyl)thieno[2,3-d]pyrimidine-2,4(1H,3H)-dione

ATP: Adenosine 5'-triphosphate

cAMP: 3',5'-cyclic adenosine monophosphate

DAB: 1,4-Dideoxy-1,4-imino-D-arabinitol hydrochloride

FRET: Förster Resonance Energy Transfer

GP: Glycogen Phosphorylase

GPCR: G-Protein Coupled Receptor

H89: N-[2-[[3-(4-Bromophenyl)-2-propenyl]amino]ethyl]-5-isoquinolinesulfonamide dihydrochloride

HCA1: Hydroxycarboxylic Acid Receptor 1

IP3: Inositol Trisphosphate

IP3R2: Inositol Triphosphate Receptor 2

LC: Locus Coeruleus

LDH: Lactate Dehydrogenase

LL: L-lactate

$[LL]_i$: Intracellular L-Lactate concentration

$[LL]_{out}$: extracellular L-Lactate concentration

MCT: Monocarboxylate Transporter

NKH: 6-[3-(dimethylamino)propionyl]-forskolin

PhK: Phosphorylase Kinase

PKA: Protein Kinase A

TCA: Tricarboxylic Acid

1. Introduction

Astrocytes are electrically non-excitable cells which are a major component of neural tissue and provide the basis of integration between neuronal, other glial and vascular cells. Astrocytic syncytia form large interconnected cellular compartments which are essential for regulation of extracellular ions, neurotransmitters, growth factors and inflammatory mediators (Colombo and Farina, 2016; Kirischuk et al., 2016). Astrocytes differ from neurones in morphology and function. Whilst electrical excitability is key for neuronal signalling, astrocytes rely on chemical transmission via G-Protein Coupled Receptors (GPCRs), protein transporters and gap-junctions to receive and integrate local signals. Astrocytes are in close association with synapses and microvasculature and regulate the extracellular space, including around synapses, providing compartmentalisation of brain space. Their roles include maintaining the correct ratio of extracellular/intracellular molecules and ions and facilitating clearance and recycling of neurotransmitters, thereby sustaining neurotransmission (Allen, 2014). However, it is now generally accepted that astrocytes participate in more complex physiological processes than acting purely as cellular "mops". They can actively undertake release, via exocytosis, channel, or transporter activity, of various signalling compounds and chemical transmitters (Kofuji and Araque, 2021; Pankratov and Lalo, 2015; Verkhratsky et al., 2016). These gliotransmitters have been implicated in a variety of physiological processes, such as long-term potentiation, memory, arousal, and depression (Gao et al., 2016; Karnib et al., 2019; Tadi et al., 2015; Zuend et al., 2020).

1.1. Astrocytes as a Metabolic Hub of the Brain

Utilisation of glucose and its metabolites from outside the nervous system is essential for brain functioning. The interface between the microvascular and the neuronal compartments is composed of microendothelial cells and astrocytes. Compared to neurons, both these cells express high levels of GLUT1 (Maher et al., 1994) – a fundamental glucose transporter found in all cell types. The high GLUT1 expression coupled with an increase in glucose uptake in astrocytes during cortical activity in vivo (Chuquet et al., 2010) indicates that astrocytes coupled to the microvasculature play an important role in supplying glucose to the brain. Understanding how astrocytes process glucose is essential for understanding how the brain handles energetic demand.

Glucose is transported into astrocytes via GLUT1 transporters down its concentration gradient. Glucose is then either trans-cellularly transported to neurones or is fed into the glycolytic cascade via hexokinase to form glucose-6-phosphate. This metabolite can be directed into a number of

metabolic pathways. From here, energy can be utilised either via continuation of the glycolytic pathway and its downstream feeding into the tricarboxylic acid cycle (TCA), or into the pentose phosphate pathway (PPP). The activity of many of the enzymes in these pathways are governed by their substrate/co-substrate concentration gradient. For example, hexokinase is inhibited by glucose-6-phosphate whilst phosphofructokinase (another important enzyme in the glycolytic cascade) is activated by ADP and inhibited by ATP (Hertz et al., 2007). As such, the level of glycolytic turnover is dependent on the balance of energetic metabolites and redox states. The metabolic destinations for glucose are displayed in *Fig1*.

Astrocytes have a unique metabolic profile. Although the metabolic pathways outlined above are generally conserved throughout mammalian cells, which pathway glucose is fed into can alter the metabolic function of cells. Pyruvate from glycolysis is either directed to the TCA or converted to lactate via lactate dehydrogenase (LDH) (*Fig1*). Conventional understanding of glycolysis in mammalian cells is that during sufficient oxygen availability (normoxic conditions), pyruvate is transferred into the TCA. Anaerobic glycolysis, where the lack of oxygen (hypoxic conditions) directs pyruvate into the conversion to lactate, is an alternative method of ATP generation. Here, the production of lactate results in the conversion of NADH to NAD^+ - fuelling earlier stages of glycolysis. This process yields significantly less ATP per glucose molecule. Astrocytes have an enzymatic metabolic profile that allows them to undertake aerobic glycolysis (*discussed below*), where pyruvate is converted to lactate in normoxic conditions. Consequently, astrocytes produce a large amount of lactate, which is released into the extracellular space (Barros, 2013). This loss of high energy metabolites would be considered an energetic disadvantage. Therefore, other explanations for lactate release have been proposed.

Astrocytes rely on glycolytic pathways. Pyruvate Dehydrogenase is the enzyme responsible for the conversion of pyruvate into Acetyl-CoA and, as such, the entry of pyruvate into the TCA cycle. This enzyme is present in astrocytes, however, seems to be highly phosphorylated, and therefore inactive (Halim et al., 2010). Further, evidence from RNA sequencing of both astrocytes and neurones found that pyruvate dehydrogenase kinase 4 transcripts are expressed at a higher level in astrocytes than in neurons (Zhang et al., 2014). This suggests that astrocytes preferentially shunt pyruvate away from the TCA cycle towards LDH activity. This reliance on the glycolytic pathway has also been shown *in vivo* via Cox10 mutant mice. Complex VI (COX) is an essential mitochondrial complex which, when lacking, forces the cells to survive only on aerobic glycolysis. Astrocytes in these mutant mice showed no histological sign of cell death after a year compared to the mice without the knockout (Supplie et al., 2017). This data is compelling in its suggestion that astrocytes are predominantly glycolytic cells.

The advantage aerobic glycolysis affords astrocytes has been explored. One explanation could be that, as shown in fig1, the TCA may be primarily used for the turnover of α-Ketoglutarate in order to process the glutamate efflux from the synaptic cleft. Therefore, the energetic needs of astrocytes must be satiated via aerobic glycolysis. Alternative explanations place emphasis on roles of lactate – the metabolic end product of glycolysis – which will be further discussed below in section *1.2. Neuronal Information Processing*

Another unique aspect of astrocytic metabolism is that they possess the enzymatic machinery to store glucose as glycogen. As such, glycogen stores are located specifically in astrocytes (Cataldo and Broadwell, 1986). Glycogen provides rapid utilisation of glucose-6-phosphate without the need for ATP – unlike the transport of glucose into the cell. Astrocyte-specific localisation of glycogen is achieved via astrocyte specific expression of glycogen interacting enzymes; glycogen phosphorylase (GP) and glycogen synthase (GYS) (Pfeiffer-Guglielmi et al., 2003). These enzymes play an important role in maintaining the rate of glycogen degradation versus synthesis. GP is interesting in the context of stimulated glycogen degradation because the kinase responsible for its activation, phosphorylase kinase (PhK), is highly regulated. The role of glycogen in brain metabolism and neuronal processing is yet to be fully established and evidence shall be covered later in this review in section *1.2.3. LL signalling in health and disease*, however this role is clearly intrinsically linked with astrocyte function and LL production.

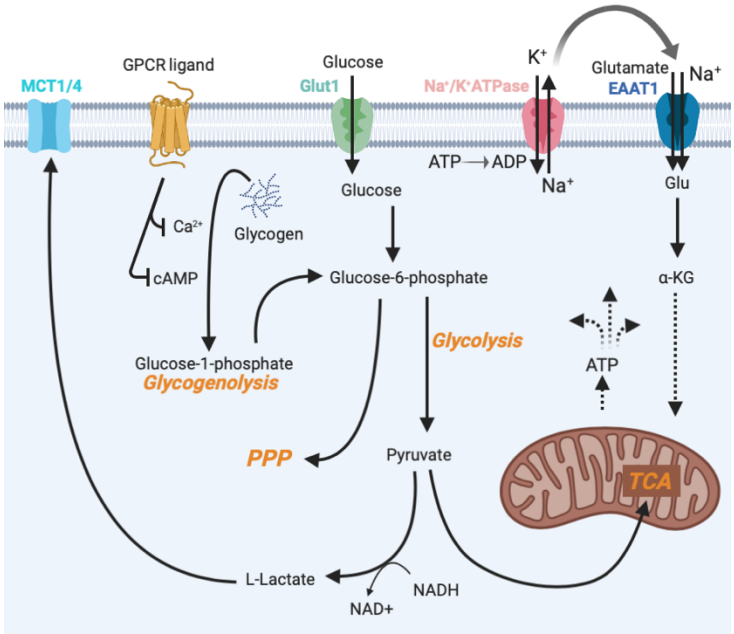

Fig 1. Metabolic destinations of glycogen and glucose in astrocytes. Na^+/K^+ATPase uses ATP to maintain a Na^+ gradient which drives the cotransport of glutamate and Na^+ via excitatory amino acid transporter 1 (EAAT1). Glutamate is either converted to glutamine or fed into the tricarboxylic acid (TCA) cycle via α-Ketoglutarate (α-KG). Glucose is transported into astrocytes via the Glucose transporter GLUT1 and converted into glucose-6-phosphate (G6P) via hexokinase. Glycogen is converted to glucose-1-phosphate via glycogen phosphorylase (GP) and subsequently to G6P. G6P is either fed into the pentose phosphate pathway (PPP) or converted to pyruvate by the glycolytic cascade of enzymes. Pyruvate is either fed into the TCA via conversion to Acetyl-coA by pyruvate dehydrogenase or converted to L-lactate by lactate dehydrogenase (LDH). This forms NAD+ from NADH which

can be used in the glycolytic cascade. This L-lactate is then transported out of astrocytes via monocarboxylate transporters 1 and 4 (MCT1/4).

1.2. Neuronal Information Processing

1.2.1. L-lactate as a means of neuronal energy support

The functional consequences of astrocytic LL release is a much-debated topic, although many studies have tried to provide an explanation. A theory which has been put forward and consequently championed by Magistretti and Pellerin is the astrocyte-neuron LL shuttle hypothesis (ANLS) (Pellerin and Magistretti, 2012). The model was originally proposed following the observation that glutamate exposure in cultured astrocytes results in lactate release (Pellerin and Magistretti, 1994). The model proposes that astrocytes at glutamatergic synapses take up glutamate with a cotransport of Na^+. This is then converted to glutamine which is transported back to neurons. The processes of glutamine synthesis and maintenance of the Na^+ concentration gradient requires ATP and pushes the energetic balance of the astrocytes in favour of glycolysis - resulting in an increase of astrocytic LL production. In fact, astrocytes contain, when compared to neurones and to the extracellular space, a higher concentration of lactate (Machler et al., 2016). These astrocytic lactate pools maintain a downward lactate gradient from astrocytes to neurons which can facilitate shuttling. Following local increase in neuronal activity and glutamatergic transmission, LL is preferentially released from astrocytes and preferentially taken up by neurones via monocarboxylate transporters (MCTs) where it is utilised for oxidative phosphorylation.

Evidence in favour of preferential release and uptake of LL from astrocytes to neurones comes from the cellular expression of different MCT isoforms in each cell type. As revealed via in situ hybridization studies, MCT2 is expressed predominantly in neurones and MCT1 and MCT4 are predominantly expressed in astrocytes (Pierre and Pellerin, 2005). This is significant because MCT2 displays kinetic properties and a higher affinity for LL, which would favour lactate uptake. *In vitro* determination of LL concentration with the Laconic sensor has established the average $[LL]_i$ as 1.4mM (Sotelo-Hitschfeld et al., 2015) – a value higher than the equilibrium constant for MCTs in astrocytes. Further, evidence for LL reservoirs in astrocytes has been shown via the use of the laconic sensor *in vivo* (Machler et al., 2016). Here, application of lactate results in a greater increase of LL in neurones than astrocytes – suggesting more LL is present in astrocytes than neurones.

There are a great number of charges levied against this model and the actual transfer of LL from astrocytes to neurones has never been directly observed *in vivo*. The limitations of all the supporting

evidence is reviewed in great depth by Dienel (Dienel, 2017). The review points out that the model doesn't account for glutamate oxidation and that glutamate stimulation of LL release is inconsistent between studies. Further, previous work using an enzymatic LL fluorescence reporter dye has suggested that astrocytic coupling via gap junctions transfers LL at a greater rate than astrocytes to neurons, a process that would restrict the build-up of LL extracellularly (Gandhi et al., 2009). Further, when measured with the Peredox fluorescence sensor, the neuronal ratio of NADH:NAD+ following neuronal stimulation increases independent of blockade of MCTs (Diaz-Garcia et al., 2017). This suggests that the energetic demand of neuronal stimulation is supplied directly by neuronal glycolysis and severely undermines the idea that LL is imported by neurones for fuel.

Whilst there is ample evidence presented for either side of the argument, the conditions in which lactate is utilised as an energy source may contribute to the discrepancies. Astrocytes are highly heterogenous cells *in vivo* and it is likely that astrocytes and neurons exhibit different metabolic behaviour dependent on brain area localisation and the inputs they receive. Further, it is also possible that the ANLS may operate under specific physiological conditions. These could include times of extreme metabolic stress and neuronal firing, such as epilepsy. Another example I would put forward could be during development when metabolism is less reliant on oxidative metabolism due to hypoxic conditions in the womb. This would be consistent with one of the arguments presented by Dienel that the genetic analysis supporting differential metabolic enzyme expression between astrocytes and neurones was done in immature neurones (Dienel, 2017).

1.2.2. L-Lactate as a signalling molecule

Whether it is used as a metabolic fuel for neurones or not, LL is clearly released by astrocytes into the extracellular compartment. Because of this, LL has been proposed a gliotransmitter (Mosienko et al., 2015). Interest into LL gliotransmission originated from the discovery of the, originally orphan, LL receptor GRP81 (Cai et al., 2008), now known as the hydroxycarboxylic acid receptor 1 (HCA1). When expressed in (CHO)-K1 cells, ^{35}S-GTPγS binding studies in conjunction with forskolin stimulation revealed that L-lactate results in $G_{i/o}$ protein-coupled inhibition of cAMP production via activation of this receptor. Also of note is the fact that D-Lactate has a weaker agonistic effect on this receptor. The existence of this receptor in the brain was confirmed by immunoreactivity studies, with highest expression levels being shown in the cerebellum and hippocampus (Lauritzen et al., 2014). The caveat with this receptor is that it requires a very high concentration of L-lactate for activation. In Lauritzen et al, the maximal concentration of 30mM only reduced forskolin-induced cAMP production in hippocampal cortical slides by ~30%. The high LL concentration needed to activate the HCA1 receptor suggests it probably has a role during supraphysiological conditions as observed during epilepsy.

There are other examples of LL signalling in the brain, for example via a novel LL receptor proposed to exist on Locus Coeruleus (LC) neurones (Tang et al., 2014). Here, exogenous LL resulted in LC neuron depolarisation with an EC50 of ~680μM. The MCT blocker 4CIN had no effect on induced depolarisation, suggesting this signalling is not metabolic in nature. Further, LL caused noradrenaline (NA) release from LC neurones, an effect which was mediated by Adenylyl cyclase (AC) activity. This effect was mimicked by optogenetic activation of astrocytes which also resulted in NA release. Therefore, at this receptor, LL acts as a gliotransmitter and has an excitatory effect on LC neurons via a G_s protein-coupled receptor. The effect is inhibited by D-lactate and, therefore, is unlikely to be mediated by HCA1. The search for this receptor is still ongoing. However, structure activity relationship studies (SAR) have explored how the structure of LL analogues effect its binding. These studies have shown the carboxyl group on LL as essential for binding. However, studying how LL binds to a number of highly expressed orphan GPCRs in LC neurons provided inconclusive results (Mosienko et al., 2018). Even without knowing the identity of this LL receptor, it is clear LL released from astrocytes does have a significant physiological role outside the scope of being an intermediate metabolic product.

LL may also interact as a signalling molecule via ion channels. High concentrations of LL potentiated NMDA receptor activation-induced Ca^{2+} currents (Yang et al., 2014). This promotes increased expression of the synaptic plasticity-related genes Arc, C-Fos and Zif268 via Erk1/2 signalling. Specifically, LL potentiates Ca^{2+} signals which are evoked by glycine/glutamate co-application – indicative of NR2B-containng NMDA receptors (Jourdain et al., 2018). As discussed before, LL enters neurones via MCTs and is converted to pyruvate via LDH. The increase in NADH acts as a reducing agent on the NMDA receptor and potentiates the pore opening (Jourdain et al., 2018). As with HCA1, the caveat with this potentiation is that it requires LL concentrations of >10mM. However, the potentiation of NMDA receptor activity indicates LL may have a role in long-term potentiation at the high end of the physiological concentration range.

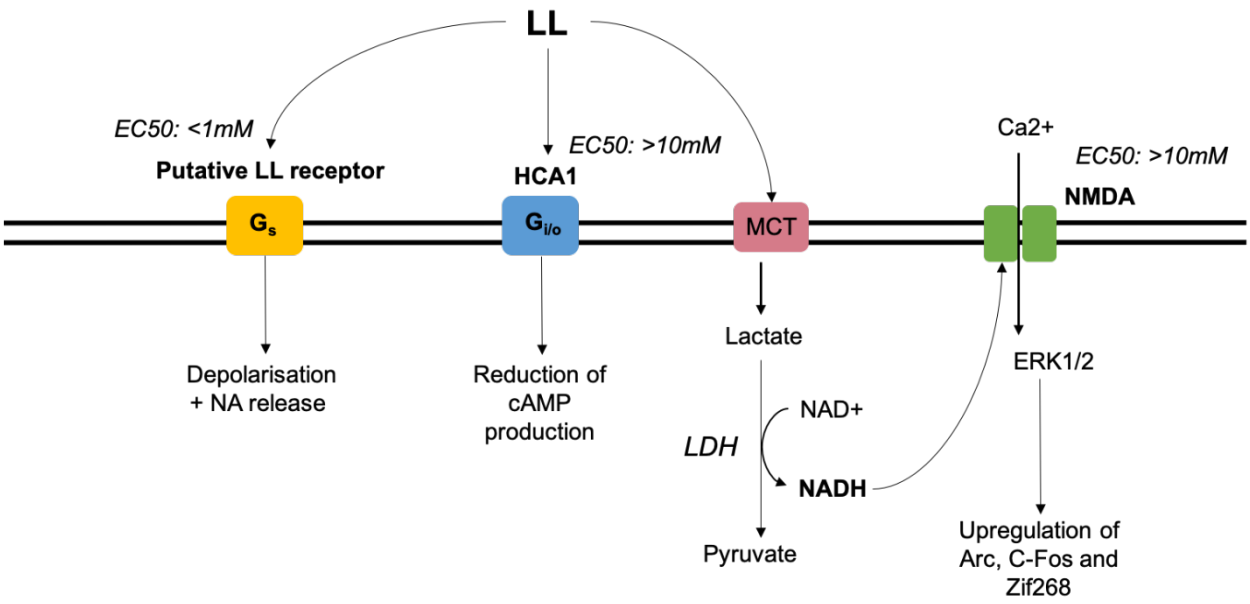

Figure 2. LL as a signalling molecule for neurones. LL can act through an unidentified Gs-coupled receptor in LC neurons resulting in depolarisation and NA release at physiological concentrations. LL can act at HCA1, a Gi/o coupled receptor, at supraphysiological concentration resulting in a reduction of cAMP production. LL can be transported through MCTs into neurons. Its conversion to pyruvate changes the redox state of the neuron and the NADH produced acts as a reducing agent on NMDA receptors. This potentiates the amount of Ca^{2+} which enters the neuron and leads to upregulation of Arc, C-Fos and Zif268 vie ERK1/2 activation.

The importance of neuronal stimulation of astrocytic LL release in neuronal functioning is quickly becoming clearer. However, the mechanisms which govern LL release are less clearly defined. Our work aims to more clearly define mechanisms for LL release.

1.2.3. LL signalling in health and disease

Astrocytic LL has been heavily implicated with long term memory formation. This memory formation has been suggested to be intrinsically linked to glycogenolysis. Using inhibitory avoidance (IA) in rats as a model for long term memory formation, application of DAB (a glycogenolysis inhibitor) resulted in disruption of long-term memory which was rescued by application of exogenous LL to the hippocampus (Suzuki et al., 2011). Further, knock down studies of LL transport via MCT1, MCT2 and MCT4 also results in disruption of long-term memory. Western blot analysis following this training exercise showed that there was also an upregulation of Arc and pCREB (genes which are upregulated

during LTP) which was inhibited by DAB application. Using this same model of memory formation, gene expression analysis has suggested genes that encode for glycogenolytic enzymes in the hippocampus are upregulated following training (Tadi et al., 2015). Further studies using IA in chicks as a study of long-term memory formation suggests that knockout of βARs in astrocytes disrupts memory formation, providing a model for a LC-astrocyte-neuron axis of memory formation based on adrenergic stimulation and its effect on release of LL (Gao et al., 2016).

The role of LL in the LC/NA axis has implications on vigilance behaviour. NA released from the LC following startle-response paradigms results in elevations of cAMP and Ca^{2+} *in vivo* (Oe et al., 2020). In different behavioural arousal paradigms, LL production and mobilisation from astrocytes has been observed (Zuend et al., 2020). Here, the rise in lactate was inhibited by both the antagonism of β adrenergic signalling and glycogen breakdown. The interplay between the LC, adrenergic signalling and LL provides is an interesting example of the effect of LL *in vivo*.

Altering astrocytic intracellular LL concentrations genetically has also been shown to alter behaviour in mice. LL production can be supressed in astrocytes using a genetically driven expression of Lactate Oxidase (LOx). When expressed in the dorsal hippocampus of mice, LOx has been shown to reduce novel-object induced freezing and increase movement in the holeboard test (Vaccari Cardoso et al., 2021). Direct alteration of LL concentrations in vivo can provide interesting insights into the physiological relevance of LL.

Interestingly, the effect of LL may have may implications pathophysiologically. Recent studies have shown that LL acts as an antidepressant in chronic social defeat stress (CSDS) mouse models of depression (Karnib et al., 2019). This was determined to be due to the alteration of levels of hippocampal class I histone deacetylase. The interaction between LL and major depressive disorder has previously been implied via the action of conventional antidepressants and upregulation of neurotrophic/growth factors (Allaman et al., 2011). Hence, it is clear that lactate in the brain has overarching functions that we are yet to fully uncover.

Uncovering the mechanisms which govern LL release is essential for further understanding into these physiological conditions.

1.3. Modulation of astrocyte metabolism by GPCR activity

Astrocytes express a wide range of G-protein coupled receptors (GPCRs). GPCRs are integral to the decoding of extracellular messages into intracellular signals. As such, they provide a perfect mechanism for stimulated LL mobilisation in astrocytes. Astrocytes exhibit robust signalling via intracellular Ca^{2+} (Bazargani and Attwell, 2016). They also exhibit signalling via cAMP, which has been implicated in a wide range of processes (Zhou et al., 2019). Both these intercellular mediators have been implicated in lactate production.

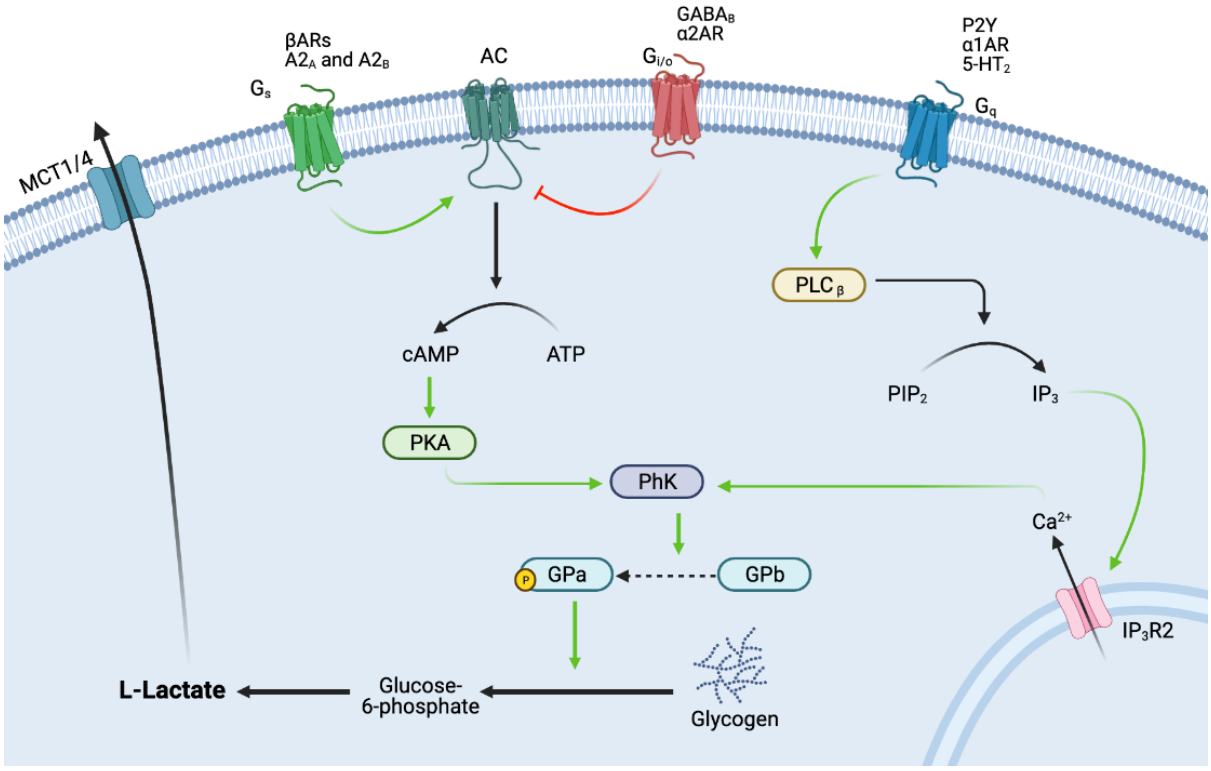

Figure 3. Schematic representation of signalling pathways involved in lactate production in astrocytes. $G\alpha_s$ and $G\alpha_i$ subunits activate and inhibit AC. This leads to the conversion of ATP to cAMP. cAMP is degraded to AMP via PDE. cAMP activates PKA. PKA phosphorylates PhK and leads to the change of GPb to its active conformation GPa. This initialises glycogenolysis, the conversion of glycogen to glucose-6-phosphate. The $G\alpha_q$ subunit activates PLC_β which converts PIP_2 to IP_3 and DAG. IP_3 activates IP_3Rs which then release Ca^{2+} from intracellular stores. Ca^{2+} binds to calmodulin which then activates PhK – feeding into the glycogenolytic activation.

1.3.1. Second messenger signalling effects on glycogenolysis

Glycogenolysis provides the perfect basis for stimulated lactate production in astrocytes. It can be stimulated independently of the metabolic equilibrium because the activation of the glycogenolytic enzymes are activated by phosphorylation. Specifically, phosphorylase kinase (PhK) governs the

activation of glycogen phosphorylase (GP). The activated GP drives the breakdown of glycogen into glucose-1-phosphate and subsequently increase the rate of glycolysis and LL production. Phk is a calmodulin dependent protein kinase with multiple isoforms which are expressed in the brain. Probably varying between isoforms, Phk is co-activated by Ca^{2+} and phosphorylation, via cAMP-dependent PKA or other phosphorylating enzymes (Nadeau et al., 2018). Therefore, any GPCR which results in an increase or decrease in either of these signalling molecules is likely to modulate glycogenolysis.

1.3.1.1. Gs coupled/Gi-coupled GPCRs

The summative activation of G_s-coupled and G_i-coupled GPCRs determines the activity levels of Adenylyl Cyclase (AC). As shown in figure 3, the $G\alpha_s$ subunit activates AC whilst $G\alpha_i$ subunit inhibits AC. AC converts of ATP to cAMP. Phosphodiesterases (PDEs) then degrade the cAMP into AMP, terminating the signal. cAMP activates protein kinase A (PKA) – the enzyme implicated in phosphorylation of PhK. Important G_s-coupled GPCRs that are expressed in astrocytes include the β1 and β2 adrenoceptors and adenosine $A2_A$ and $A2_B$ receptors. In the case of the β-adrenoceptors, there has been evidence in cultured astrocytes of the glycogenolytic effect of β-adrenergic agonists (Subbarao and Hertz, 1990). An alternative view presented by Xu et al., suggest that β-adrenergic activation results in a PKA mediated G_s/G_i switch which results in an increase in Ca^{2+} (Xu et al., 2014). There is clearly significant cross talk throughout the signalling cascades. However, glycogenolysis is clearly affected by the activity of AC-interacting GPCRs.

1.3.1.2. Gq coupled GPCRs

The emphasis on Ca^{2+} signalling due to the calmodulin sensing domain on PhK has driven research into the effects of G_q-coupled receptors. As shown in figure 3, the $G\alpha_q$ subunit activates phospholipase C (PLC) which converts phosphatidylinositol 4,5-bisphosphate (PIP2) into inositol triphosphate (IP3) and diacylglycerol (DAG). The production of IP3 activates IP3 Receptors which then release Ca^{2+} from intracellular stores. The released Ca^{2+} binds to calmodulin and activates PhK. Gq receptors expressed in astrocytes include P2Y ATP-activated receptors, α1 adrenoceptors and 5-HT_2 receptors. They have all been shown to stimulate glycogenolysis in culture (Sorg et al., 1995; Subbarao and Hertz, 1990; Zhang et al., 1993). Clearly, Ca^{2+} is essential for glycogenolysis. Astrocytic glycogenolysis is probably a summation of cAMP and Ca^{2+} signalling and its effects on glycogenolytic enzymes. Due to the connectivity of astrocytes in neural tissue, astrocytes more likely act as coincidence responders in which activation of multiple GPCRs 'compete' or synergise for an effect on glycogenolysis.

1.3.2. Modulation of LL production by GPCRs

Direct observation of the effect of GPCR signalling on LL production is sparse. However, more recently, the effect of adrenergic and cAMP signalling following GPCR activation has been observed using the Laconic nanosensor (Fink et al., 2021; Horvat et al., 2021; Vardjan et al., 2018). These studies paint a complex picture of the effect of cAMP and Ca^{2+} on LL production. Vardjan et al., showed that application of the HCA1 agonist, 3Cl-5OH-BA, resulted an increase in $[cAMP]_i$ and consequently $[LL]_i$. Conversely, Horvat et al., using a mix of $\alpha 1/\beta$ adrenoceptor (AR) agonists (isoprenaline and phenylephrine) showed that activation of βARs (G_s-coupled) alone was not sufficient in producing an increase in $[LL]_i$. However, activation of both the $\alpha 1$ (G_q-coupled) and βARs did produce a significant increase in $[LL]_i$. Therefore, they conclude that the Ca^{2+}-signalling stimulated by G_q-protein signalling is essential for LL production. In Fink et al, the authors use high concentrations of agonist, for example, 200μM NA. Despite arguments that local concentrations of neurotransmitters can be much higher, this is beyond the conventionally stated physiological concentration of endogenous NA. However, receptor kinetics and expression may influence the interpretation of the effect of GPCRs on LL production. We aim to bypass these complications by directly stimulating adenylyl-cyclase (AC) with the forskolin-derivative, NKH.

1.4. $GABA_B$ receptor signalling in astrocytes

Astrocytes express a wide variety of GPCRs. Interestingly, there is evidence of these GPCRs exhibiting different signalling and physiological roles when compared to their expression in neurones. For example, in astrocytes, $GABA_B$ signalling has been shown to induce long lasting Ca^{2+} oscillations (Mariotti et al., 2016). Other canonical $G_{i/o}$-protein coupled receptors such as the CB1 receptor have been shown to induce Ca^{2+} signalling which have been implicated in synaptic plasticity (Rasooli-Nejad et al., 2014). This has been proposed to occur via G_q-protein coupling (Navarrete and Araque, 2010). The mechanism behind $GABA_B$ mediated Ca^{2+} oscillations remains unclear, although they have been shown to be dependent on IP3R activation. Interneuron-mediated synaptic potentiation in hippocampal CA1-CA3 neurones has been shown to be a product of $GABA_B$-mediated Ca^{2+} oscillations in astrocytes (Perea et al., 2016), an effect dependent on glutamate release from astrocytes. This effect was only observed during burst firing of interneurons. As such, this illuminates a mechanism in which astrocytes switch inhibitory signals from interneurons into excitatory signals during periods of sustained interneuron firing. Further, *in vivo* stimulation via ChR2 of PV and SST interneurons resulted in differential potentiated Ca^{2+} responses in neighbouring astrocytes (Mariotti et al., 2018). Physiologically, astrocytic knockdown of $GABA_B$ receptors in the PFC disrupts cognition

in mice; an effect which can be restored by optogenetic activation of astrocytes in the mPFC (Mederos et al., 2021). Cognition enhancement following optogenetic activation was inhibited by mGlu1 (G_q-protein coupled) receptor antagonism, suggesting release of glutamate following $GABA_B$ activation is responsible. Thus, astrocytic gliotransmission via $GABA_B$ signalling may play an important role in neural coding.

Given the implications of astrocytic $GABA_B$ signalling on neuronal signalling, and the implications of astrocytic LL release on neuronal signalling, we wanted to explore how $GABA_B$ signalling effects LL mobilisation (both production and release). We approached this by measuring intracellular LL with the FRET-based biosensor Laconic and measured the extracellular LL concentration with an EnzyFluo LL assay kit. Using the $GABA_B$ agonist, baclofen, we aimed to determine the effects of $GABA_B$ activation on LL mobilisation in both basal and stimulated conditions. Using NKH and a variety of other pharmacological agents, we also aimed to further clarify the mechanisms which govern stimulated LL mobilisation. Our working set of hypotheses were:

- AC-activity stimulates production and release of astocytic LL.
- $GABA_B$ activity regulates the production and release of astocytic LL.

Our results suggest that $GABA_B$ activation negatively regulates LL mobilisation in astrocytes.

2. Methods

2.1. Primary astrocyte culture

2.1.1. Preparation of cultures

Primary astrocyte cultures were obtained via a protocol adapted from Marriott, Hirst & Ljungberg (1995). A Wistar rat P2 pup was terminally anaesthetised with 5% isoflurane and decapitated using sharp scissors. The brainstem and mid-brain were dissected, chopped and agitated in trypsin (0.05% with EDTA; Invitrogen, 25300-054) for 15 minutes. The addition of 15ml full culture media (*see table 1*) terminated the trypsination process, after which the cell suspension was centrifuged at 1000rpm for 5 min. The supernatant was aspirated and the cell pellet was resuspended in 40ml HBSS (Hanks Balanced Salt Solution; Invitrogen, 14175- 129). Containing 10ml of DNase I: 0.04mg/ml Deoxyribonuclease I (DNase I, from bovine pancreas; Sigma, D5025). When the cell suspension settled, the supernatant was collected and reserved. The process was then repeated two more times and the remaining supernatant was collected and combined. The combined cell suspension was

strained through a 40μm cell filter and centrifuged at 1000rpm for 5min. The supernatant was then aspirated and the pellet was resuspended in full culture media, seeded in a T75 flask, and incubated for 7 days at 37˚C with 5% CO2 in. For the removal of microglia and oligodendrocytes, the culture was gently shaken overnight and the media was removed and replaced with fresh media. The culture was kept in the incubator for use for up to 21 days after preparation.

Table 1. Composition of full astrocyte culture media.

Component	**Amount**
DMEM (Invitrogen, 61965-059)	89%
Foetal bovine serum (FBS, Invitrogen, 10108-165)	10%
Streptomycin/Penicillin (Pen/Strep, 10,000 U/mL, Invitrogen, 15140-122)	1%

2.1.2. Cell passaging

Astrocytes were incubated in culture media in T75 flasks at 37˚C with 5% CO_2. For plating, cells were washed with 10ml DMEM and detached from the culture plate via trypsinization (Trypsin, 0.05% (1x), Invitrogen) at 37˚C for 4 mins. Following this, trypsin was neutralized with 5ml of FBS-containing media and pelleted for 5mins at 1000 rpm. The supernatant was aspirated, and the pellet was resuspended in 10ml culture media. Astrocytes were then plated at $1x10^5$ cells/well in 24-well plates (for lactate release assay) or on collagen coated glass coverslips (13mm) inserted into the plates (for confocal imaging). To determine the concentration of astrocytes in cell suspension, a haemocytometer was charged with 10μl of a 1:2 dilution of the suspended pellet. The cell counts in the 4 outer squares of the haemocytometer chamber were converted into a concentration as follows:

$$\frac{Cell\ count}{4} \times 2 \times 10^4$$

The volume of cell suspension needed for plating was then calculated by:

$$\frac{(well\ volume \times no.wells) \times 10^5}{calulated\ cells/ml}$$

Any remaining cell suspension was placed back into a T75 and incubated.

2.2. Adenovirus Production

2.2.1. Cotransfection

Viral vectors were produced via recombination of shuttle plasmids (pXCX) which contained the required cassette with a helper plasmid (pBHG10) which contained the majority of adenoviral genome. The helper plasmid is an altered adenoviral genome as such that it is missing the E1 and E3 genes (Bett et al., 1994), allowing replication of viral vectors only in E1/3 gene product containing HEK293 cells (Graham and Prevec, 1995). Initially, 5µl shuttle plasmid and 5µl helper plasmid were placed in an aliquot with 400µl of DMEM. 20µl of FuGENE reagent was then added and vortexed gently. The solution was incubated at RT for 5min and then added to a T25 flask containing 60-70% confluent HEK293 cells. These cells were kept at 5% CO2 at 37ºC and observed periodically until cytopathic effect (CPE) was seen. More DMEM was added to the cells if the solution in the flask showed discolouration, in order to prevent acidity induced cell death. Once full CPE was observed, the flask was placed into the freezer at -20ºC in order to lyse the cells and release the viral vector.

2.2.2. Reinfection

The flask was removed from the freezer and defrosted at RT. The solution was centrifuged for 5min at 1000rpm. 500µl of the supernatant was added to a T25 flask containing 60-70% confluent HEK293 cells and they were placed in the incubator as before. The remaining supernatant was reserved at -20ºC. This process (CPE observation, freezing and reinfection) was repeated until the CPE occurred within 2/3 days. 1ml of this viral supernatant (following freezing, defrosting and centrifuging) was then used to infect a T75 flask containing new HEK293 cells.

2.2.3. Bulking up

The viral supernatant collected from the T75 flask was used to infect 10 T150 flasks containing 60-70% confluent HEK293 cells (1ml supernatant per flask). When CPE was observed the cell suspension from all the flasks was collected and centrifuged at 1000rpm for 5min. The supernatant was aspirated and pellets were resuspended and combined, concentrating the viral vector-containing cellular suspension. The final pellet from all the flasks was resuspended in 2.5ml of 0.1M Tris-HCl (Sigma, T-5941) at a pH of 8 and frozen at -20ºC.

2.2.4. Purification

The 2.5ml Tris-HCl cellular suspension was defrosted and kept on ice. The solution was then sonicated to release the remaining viral particles. The suspension was sonicated for 45sec and placed on ice for 1min. This was repeated 4 times. The solution was placed in the centrifuge at

3000rpm and 4ºC for 10min. The supernatant was used for further purification and the cell debris was discarded. 1 part viral suspension was added to 0.6 part solution of saturated Caesium Chloride (CsCl; Invitrogen, 15507-023) diluted in 0.1M Tris-HCl at pH 8. The solution was placed into an ultra-centrifuge (UCF) tube and topped up with 0.6ml saturated CsCl solution. The tube's weight was recorded and the process was repeated with another UCF tube without viral suspension. Once the tubes were counterweighted, they were sealed and placed in the ultracentrifuge overnight at 50,000rpm at 15ºC. The following morning, the viral band which formed was collected. A 5ml syringe with needle attached was used to pierce the tube and collect the viral band. A second needle and syringe was used to pierce the top and provide a release of pressure. The viral band was transferred into a new UCF tube and saturated CsCl diluted in 0.1M Tris-HCl was added until the tube was full. Following counter weight with another UCF tube, the tubes were placed into the ultracentrifuge for 4hours at 50,000rpm at 15ºC. Before the 2nd ultracentrifugation step was completed a PD-desalting column (GE Healthcare, 17-0851-01) was prepared for collection of viral vector. 25ml of 10mM Tris/$MgCl_2$ (Qbiogene, MGCL0500) was passed through to calibrate the column. 3ml of the viral band was collected as before with needle and syringe and added to the column. After the addition of 0.5ml Tris/$MgCl_2$, a further 2.5ml of Tris/$MgCl_2$ and the viral solution was collected from the column. The viral vector containing solution was then filtered through a 0.22μm syringe filter and transferred at volume of 20μl to aliquots. The aliquots were placed in the freezer at -80ºC until use.

2.2.5. Titration

A 12-well plate of 90% confluent HEK293 cells was incubated at 37ºC and 5% CO_2 for 48hours with 100μl/well of serial viral vector suspension from concentrate to 10^{-8}. On the day of the titration, the media from the 12-well was aspirated and left to dry for 10mins. 1ml of methanol was added per well and placed in the freezer at -20ºC for 15mins to fix the cells. Methanol was aspirated and the wells were washed with 1ml of a solution of phosphate buffer solution (PBS; Fisher Scientific, BR0014G) /1% bovine serum albumin (BSA; Sigma, A9647) 3 times. Wells were incubated at 37ºC for 1hour with 500μl of 1000x diluted anti-adenovirus hexon protein (Biodesign, B65140G).The wash procedure was then carried out. Wells were then incubated at 37ºC for 1 hour with 500μl of secondary horseradish peroxidase (HRP)-conjugated antibody (Zymed, 81-1620) diluted 500x. The wash procedure was repeated before addition of 3,3-Diaminobenzidine (DAB) solution. Addition of 1 tablet of DAB (0.7 mg/mL; Sigma, D4293) to 15ml of distilled water was done in the absence of light to avoid photodegradation. A second tablet of urea hydrogen peroxide (2 mg/mL; Sigma, U1380) was added and shaken. 500μl of this solution was added to the wells in the dark. Once dark products started to form, an average count was calculated from the dark cells recorded from 5 fields of view. The titre was then calculated with this equation:

$$\frac{Average\ count\ stained\ cells\ \times 157}{Vol.\ virus\ (ml) \times dilution\ factor)}$$

2.2.6. Viral Transduction

Astrocytes were plated on collagen coated 13mm coverslips at 1x10^5 cells/ml and transduced via addition of adenoviral vectors into the culture media. Volume of adenovirus used was calibrated via calculation of the multiplicity of infection (MOI). The MOI was optimized to a value which provided the most efficient transduction. They were left to incubate for 3 days before use. Expression efficacy was monitored following transduction.

2.3. Confocal Fluorescence Imaging

2.3.1. Fluorescent reporters

2.3.1.1. AVV-CMV-Laconic

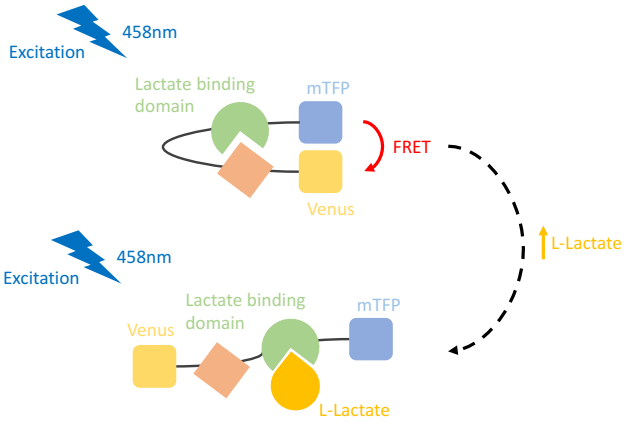

Figure 4. Representation of Laconic sensor in absence or presence of LL. Conformational change in response to LL binding reduces FRET and changes the ratio of fluorescence intensity between the fluorophores.

The Laconic sensor reports intracellular lactate concentration using Förster resonance energy transfer (FRET) between a mTFP fluorophore (emission peak: 492nm) and a Venus fluorophore (emission peak: 526nm) (San Martin et al., 2013). When excited at 458nm in the absence of LL, the proximity of the 2 fluorophores allows photon donation due to FRET from the mTFP fluorophore to the Venus fluorophore. This means the ratio between the emission spectra of each fluorophore is low. Following binding of LL, the movement of the fluorophores away from each other decreases the transfer of photons from mTFP fluorophore to the Venus fluorophore and increases the ratio, indicating an increase in intracellular lactate concentration *(fig 4).* The laconic sensor was delivered to astrocytes via AVV with a CMV promoter to allow expression in primary astrocyte cultures (AVV-CMV-Laconic).

2.3.1.2. AVV-sGFAP-mT2-Epac-cpVcpV(H187)

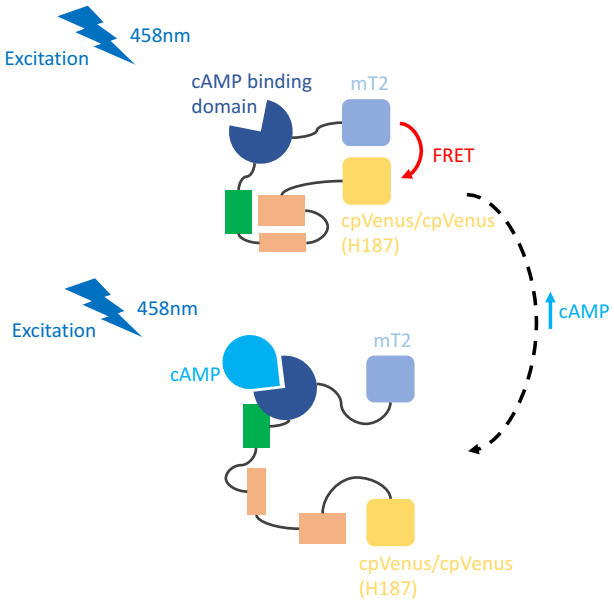

Figure 5. Representation of EPAC sensor in absence or presence of cAMP. Conformational change in response to cAMP binding reduces FRET and changes the ratio fluorescent intensity between the fluorophores

The EPAC cAMP sensor reports intracellular cAMP dynamics though FRET-based ratiometric imaging in a similar manner to the Laconic sensor (Klarenbeek, Goedhart, van Batenburg, Groenewald & Jalink, 2015). When excited at 458nm in the absence of cAMP, FRET occurs between MT2 (emission peak: 480nm) and cpVenus/Venus(H187) (emission peak: 530nm). Like Laconic, binding of cAMP results in an increase in the fluorescence intensity of the attached fluorophores. The construct is delivered via AVV with a sGFAP promoter. This promotes expression in sGFAP positive astrocytes.

2.3.2. FRET sensor recording

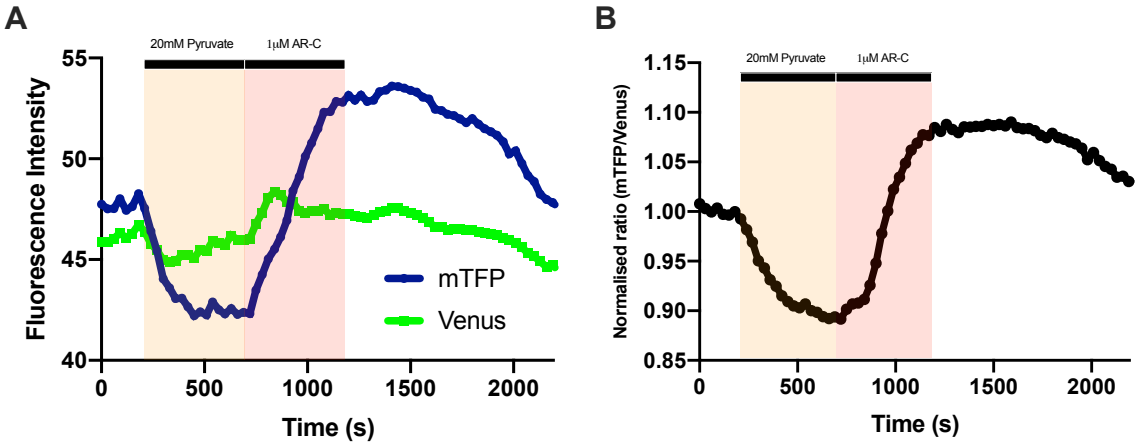

Fig6. A) Representative trace of the fluorescence intensity of the individual fluorophores with the Laconic sensor in response to application of 20mM pyruvate followed by 1µM AR-C. **B)** Ratio of mTFP/Venus fluorescence corresponding to A. Pyruvate caused trans-acceleration of lactate out of the cell, followed by intracellular lactate build up when MCTs were blocked with AR-C.

A Leica SP-2 upright confocal laser scanning microscope was used for live cell imaging of astrocytes expressing biosensors. The recording chamber was continuously superfused at 2ml/min with HEPES-buffered solution (HBS); *see table 2*. The chamber was kept at a constant 31.8°C. The coverslip was placed directly into the chamber. At 1min, the peristaltic pump was stopped briefly, and the chamber input tube was transferred to a new solution containing drug at required concentration. After 9min, the tube was transferred back to the HBS solution for a following 11 min. Total time of recording was 20 min. Both sensors were excited at 458nm with an Argon ionised laser. The fluorescence was measured with 10x and 20x water immersion lenses and sampled xyt mode at 0.05 Hz (20sec). Both the Laconic and EPAC sensor's emission spectra were measured at wavelength bands of 465-500nm/515-595nm. Recording was undertaken with Leica software. Within the Leica software, regions of interest (ROIs) where selected and the quantitative change in fluorescence was exported. The data were analysed in Excel.

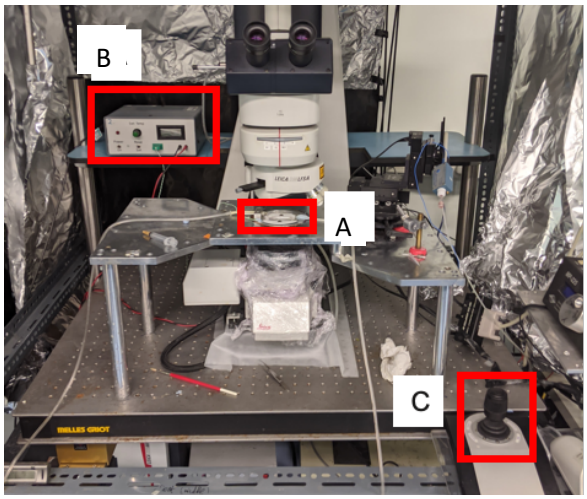

Fig7. Leica SP-2 upright confocal laser scanning setup. **A**: tissue chamber with HBS perfusion. **B**: Thermostat heat controller **C**: Control stick used to control the position of the stage.

Component	Concentration (mM)
NaCl	137
KCl	3 (for laconic) OR 5.4 (for EPAC)
$NaHCO_3$	0.34
KH_2PO_4	0.44
$CaCl_2$	1.67
MgSO4	0.8
NaHCO3	4.2
HEPES	10
Glucose	2 (for laconic) OR 5.5 (for EPAC)

Table 2. Components and corresponding concentrations used for HEPES-buffered solution (HBS).

2.4. Fluorometric measurement of LL release

Quantification of LL in conditioned media was undertaken using a LL EnzyFluo Assay Kit (BioAssay Systems, EFLLC-100). This kit allows the quantification of LL via LDH oxidation. The NADH produced as a by-product converts the supplied probe into a fluorescent product with λex/em = 530/585nm. Astrocytes were plated in a 24-well plate in culture media at a concentration of $1x10^5$ with a total volume of 0.5ml three days prior to drug application and media collection. To stimulate LL release, drugs diluted in DMEM were added for 15. To assess basal release for 15 min, media was replaced with DMEM with or without glucose or DAB. The conditioned DMEM was collected and stored at -20°C until processed.

For determination of extracellular LL, samples were thawed and diluted 5 times. 50uL of each sample were placed in a well of a 96-well black plate and 50uL of assay kit solution were added to the wells and left to incubate in the dark for 1 hour at room temperature. Measurements were taken in a microplate reader (Tecan i-2000) and referenced to a calibration curve *(Fig 8):*

$$[Lactate](\mu M) = \frac{F_{sample} - F_{blank}}{Slope} \times 5$$

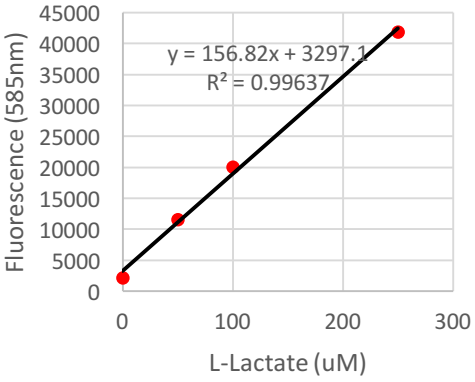

Fig 8. Example calibration curve for determining the L-lactate concentration in the sample. The LL 0uM was subtracted from the sample value and the slope = 156.82 was used

Results from this assay were normalised using the following equation:

$$\Delta\,[lactate]\;from\;control = \left(\frac{[lactate\;in\;condition\;on\;same\;plate]}{[lactate\;in\;control\;well\;of\;plate]} \times 100\right) - 100$$

This was used to account for the variability in [LL] in the control between the different assay plates.

2.5. Drugs

All compounds were ordered as solid and stock solutions were prepared in ddH2O unless indicated otherwise and stored at -20C until use: **NKH 477** (6-[3-(dimethylamino)propionyl]-forskolin, Sigma-Aldrich, N3290) [10mM], **Baclofen** ((*RS*)-4-Amino-3-(4-chlorophenyl)butanoic acid, Tocris Biosciences, 0417) [10mM], **DAB** (1,4-Dideoxy-1,4-imino-D-arabinitol hydrochloride, Sigma-Aldrich,

D1542) [10mM], **AR-C155858** (6-[(3,5-Dimethyl-1H-pyrazol-4-yl)methyl]-5-[[(4S)-4-hydroxy-2-isoxazolidinyl]carbonyl]-3-methyl-1-(2-methylpropyl)thieno[2,3-d]pyrimidine-2,4(1H,3H)-dione, Tocris Biosciences, 4960) [1mM], **H89** (N-[2-[[3-(4-Bromophenyl)-2-propenyl]amino]ethyl]-5-isoquinolinesulfonamide dihydrochloride, Tocris Biosciences, 2910) [10mM].

2.6. Statistical Analysis

For confocal data, the data were normalised to the first 60sec of baseline recording. For LL release, data were calculated as percentage change from the control condition on the same assay. Linear regression was used for the calibration curve. All error bars are plotted as ±SEM. All data were organised and normalised in Excel. The data were then plotted and statistical analysis was carried out in Graphpad Prism. The type of statistical analysis stated in the figure legends. Statistical tests were chosen dependent on the variance and normality in each of the groups. Parametric ANOVAs were chosen if the data had equal variance between groups and the data was normally distributed within groups. Non-parametric Kruskal-Wallis tests were chosen if the previous parameters were not satisfied. The D'Agostino-Pearson K^2 test was used to assess the normality within groups. Multiple comparisons specific to the analysis of variance used were used to compare means between groups. Significance is recorded at $p=<0.05$.

3. Results

3.1. Baseline LL mobilisation

3.1.1. Gi/o-protein activation by baclofen decreases basal LL production but does not affect release

Basal intracellular LL levels as measured with Laconic were not significantly affected by 100μM baclofen. In order to address the possibility that LL release was masking the effect of baclofen on basal production, we repeated baclofen stimulation in presence of the MCT blocker AR-C. When blocking LL release via MCTs, the intracellular build-up of LL can be attributed to the basal rate of production. 1μM AR-C resulted in an increase in intracellular LL ($[LL]_i$). Application of both 10μM and 100μM Baclofen in combination with 1μM AR-C significantly decreased the change in $[LL]_i$ compared to AR-C alone *(fig7).* There was no significant difference between 1μM AR-C + 10μM baclofen and 1μM AR-C + 100μM baclofen, suggesting the concentrations at which baclofen exhibits its maximal effect is 10μM or below. These results indicate that basal LL production is driven by constitutive AC activity.

The $GABA_B$ receptor agonist baclofen in the concentration range 1μM to 100μM had no measurable effect on baseline LL release ($[LL]_{out}$) as sampled over 15 min when compared to control *(fig8).* We can, therefore, discount the possibility that $GABA_B$ activation causes LL release.

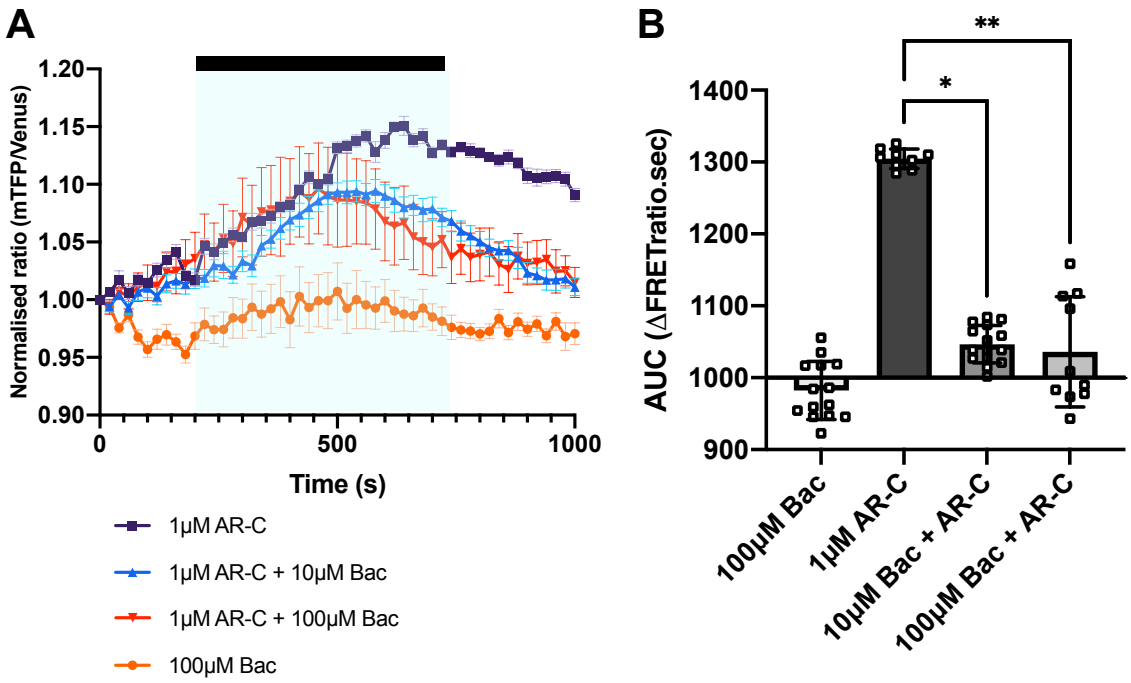

Fig7. $G_{i/o}$ activation by baclofen decreases LL production in astrocytes under baseline conditions and this effect is unmasked when LL release is blocked. A. Normalized Laconic FRET ratio in response to 1μM AR-C (n=10, c/s 2), 1μM AR-C + 10μM baclofen (n=15, c/s 2), 1μM AR-C + 100μM baclofen (n=15, c/s 2) and 100μM baclofen (n=14, c/s 2) **B.** Calculated AUC over 1000sec in response to drug application. Kruskal Wallis (Dunn's Multiple Comparison) was used to compare the means of 1μM AR-C + 10μM baclofen and 1μM AR-C + 100μM baclofen against 1μM AR-C. Significance asterisks are defined at: * = p≤0.05, ** = p≤0.01.

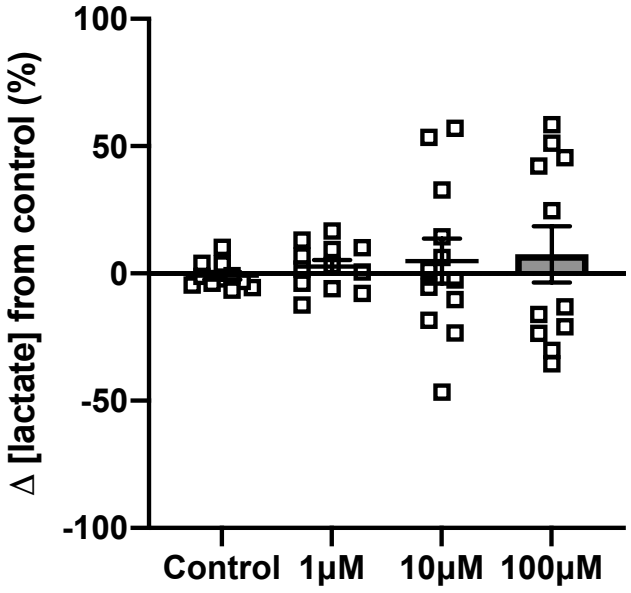

Fig8. $G_{i/o}$ activation by baclofen does not significantly affect baseline LL release in cultured astrocytes. $[LL]_{out}$ calculated using EnzyFluo assay during 15min incubation. All conditions: n=12. Kruskal-Wallis (Dunn's multiple comparisons) used to compare all groups to control.

3.1.2. Glycogen contributes to basal LL mobilisation

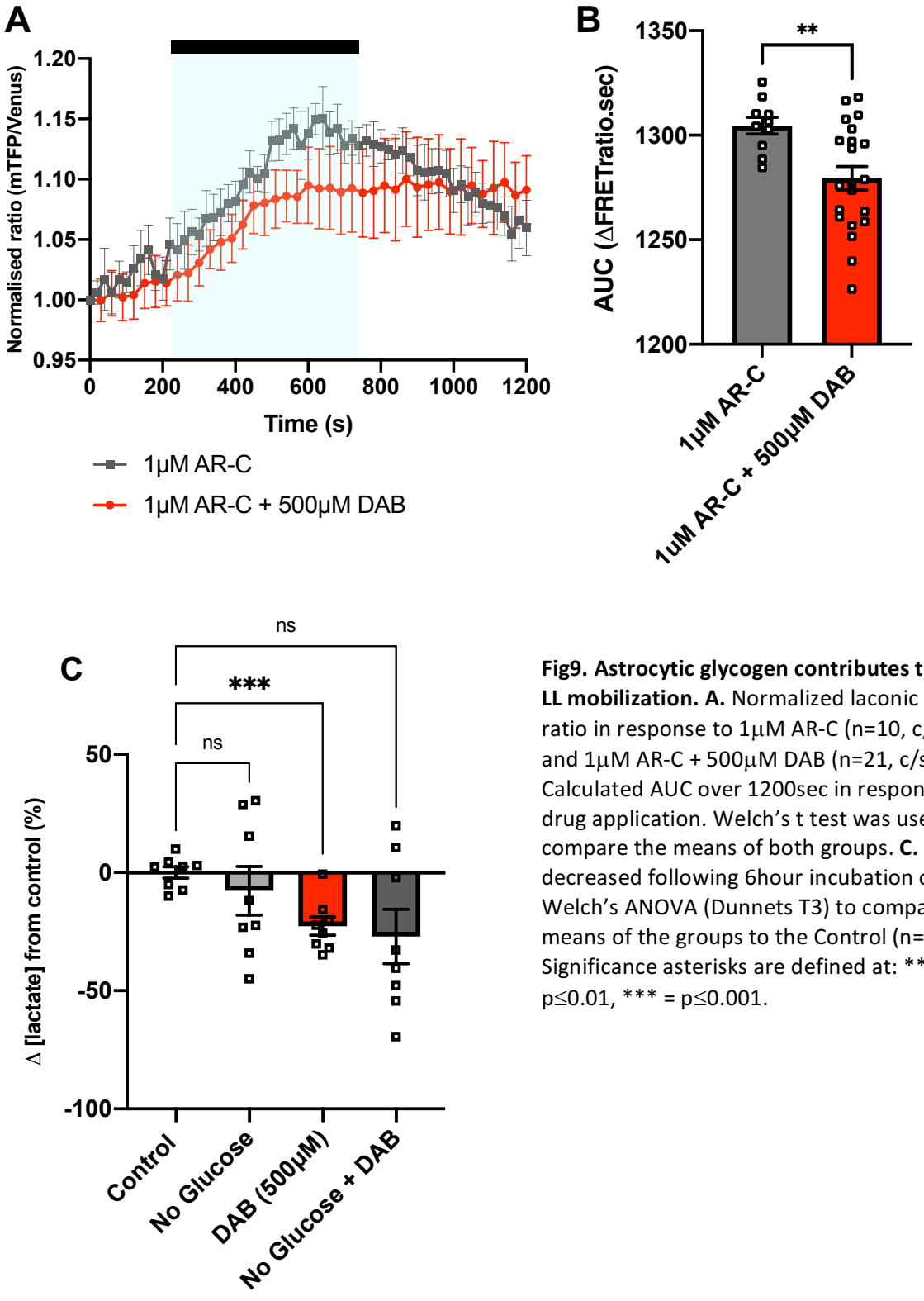

Fig9. Astrocytic glycogen contributes to basal LL mobilization. A. Normalized laconic FRET ratio in response to 1µM AR-C (n=10, c/s 2) and 1µM AR-C + 500µM DAB (n=21, c/s 2). **B.** Calculated AUC over 1200sec in response to drug application. Welch's t test was used to compare the means of both groups. **C.** $[LL]_{out}$ is decreased following 6hour incubation of DAB. Welch's ANOVA (Dunnets T3) to compare the means of the groups to the Control (n=8). Significance asterisks are defined at: ** = $p \leq 0.01$, *** = $p \leq 0.001$.

In order to better understand the mechanisms regulating the astrocytic LL pool under unstimulated conditions, we determined the contributions of glycogen turnover and of glucose import to basal LL

production. Pre-incubation with 500µM DAB resulted in a decrease in LL build-up as reported by the Laconic FRET signal compared to 1µM AR-C alone *(fig9B).* This suggests that glycogenolysis plays a role in upholding basal intracellular LL pools. LL release was also decreased following DAB application. Over a 6 hour incubation period, Incubation with 500µM DAB resulted in decrease in LL release compared to control *(fig9C*). Incubation with no glucose media did not show a significant difference in LL release when compared to control and this can be attributed to the greater variation shown in release *(fig9C)*. Similarly, incubation with no glucose media and 500µM DAB also showed no significant change from control *(fig9C).* This suggests that basal LL release is, at least in part, dependent on glycogen turnover.

3.2. Section 2: Stimulated LL mobilisation

3.2.1. $G_{i/o}$-signalling by baclofen inhibits AC activity in astrocytes

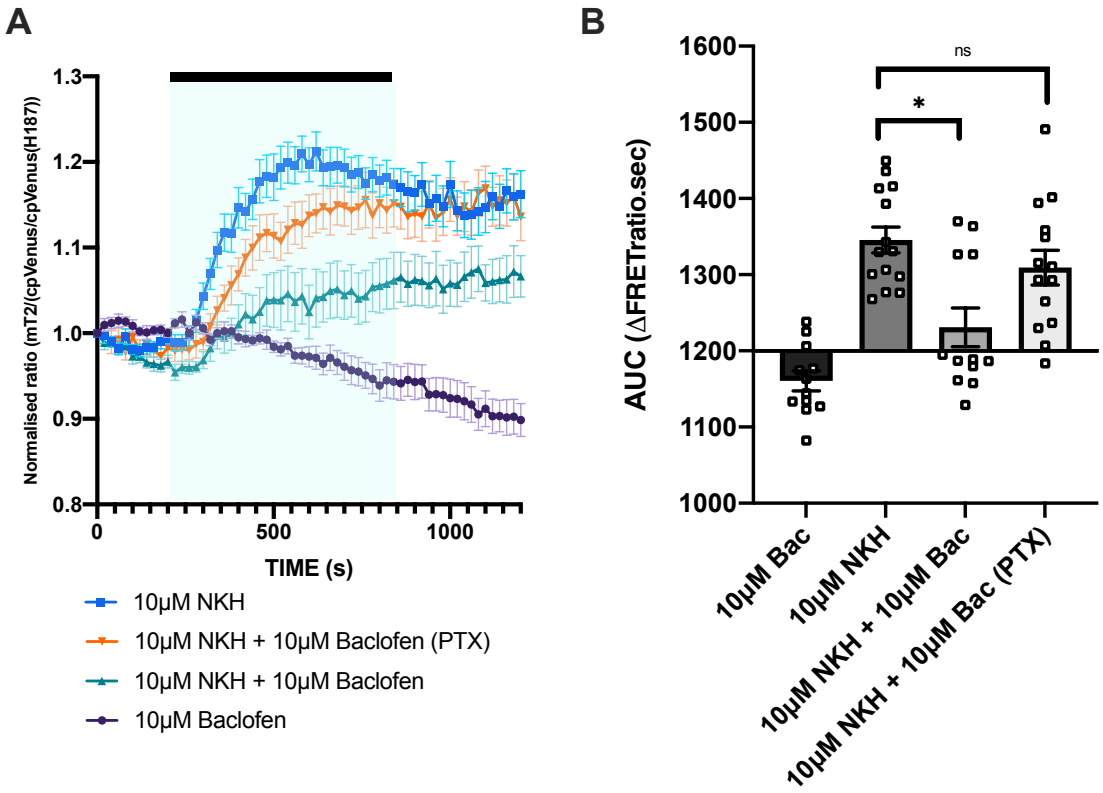

Fig10. Baclofen reduces NKH-stimulated cAMP production. A. normalized EPAC FRET ratio in response to 10µM Baclofen (n=13, c/s 2), NKH 10µM (n=10, c/s 2), 10µM NKH + 10µM Bac (n=12, c/s 2) and 10µM NKH + 10µM Bac with pre-incubation with PTX (n=12, c/s 2). Application between 210-750sec. **B.** Calculated AUC over 1200sec in response to drug application. One-way ANOVA with post-hoc multiple comparisons to compare the means of the groups to each other. Significance asterisks are defined at: * = p≤0.05.

In order to determine the effect of $GABA_B$ receptor activation on basal and stimulated AC-dependent cAMP production, we used the EPAC FRET sensor. Baclofen (10µM) resulted in a gradual decrease in cAMP signal, consistent with inhibition of AC activity. As expected, the forskolin analogue NKH (10µM) increased cAMP. When AC activity was elevated by NKH, coapplication of baclofen inhibited cAMP production as expected for $GABA_B$ receptor activation/$G_{i/o}$-protein signalling. Blocking $G_{i/o}$-proteins by pre-incubation with pertussis toxin (PTX) inhibited the effect of baclofen on NKH-stimulated cAMP production, blocking the effect of baclofen. This data confirms that baclofen inhibits the NKH-stimulated cAMP production, as expected of a $G_{i/o}$-GPCR agonist. Both NKH and baclofen effects outlasted the duration of the recording so must have sustained effects on cAMP at this application length.

3.2.2. AC activity stimulates LL mobilisation

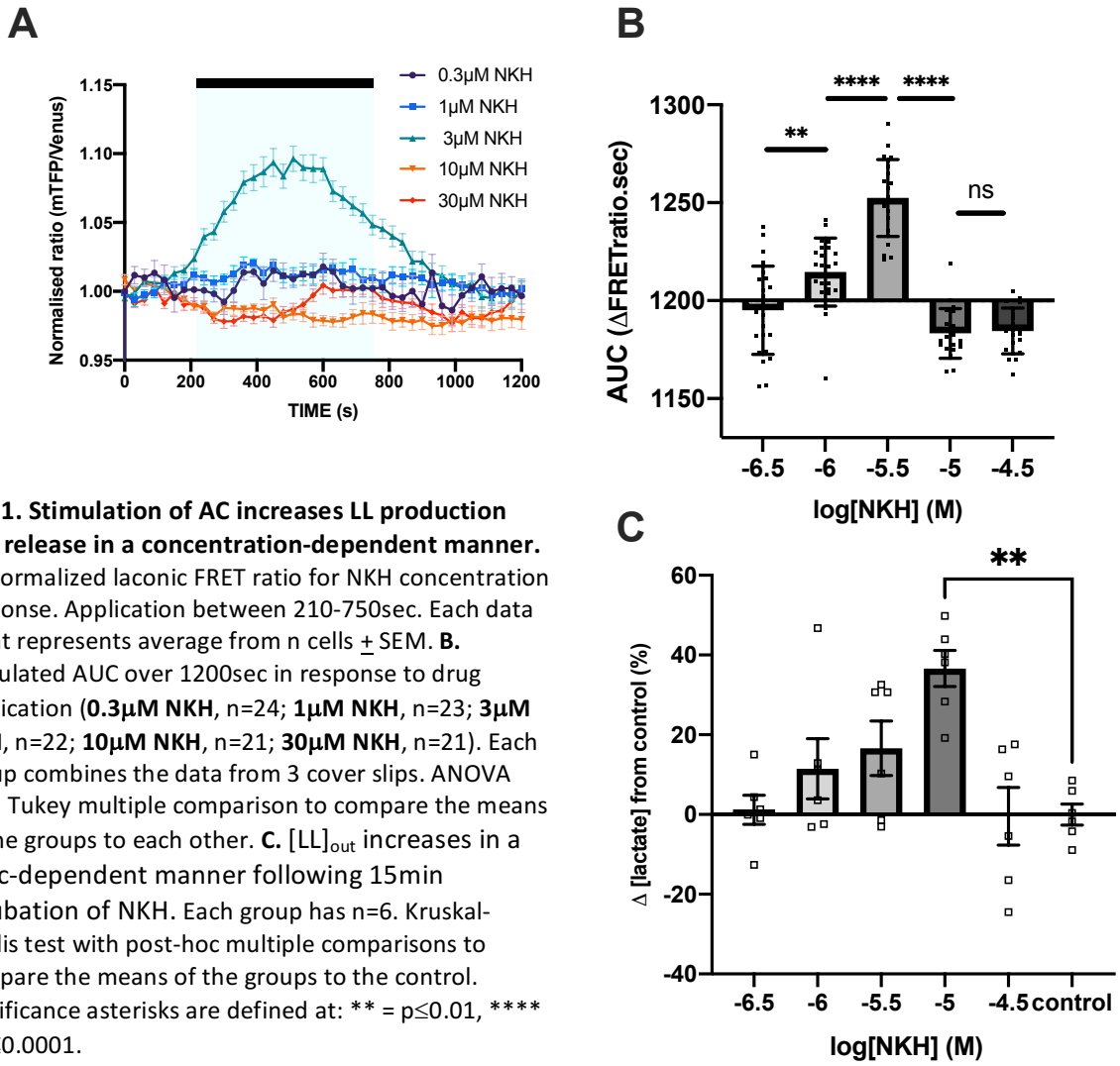

Fig11. Stimulation of AC increases LL production and release in a concentration-dependent manner. **A.** Normalized laconic FRET ratio for NKH concentration response. Application between 210-750sec. Each data point represents average from n cells ± SEM. **B.** Calculated AUC over 1200sec in response to drug application (**0.3µM NKH**, n=24; **1µM NKH**, n=23; **3µM NKH**, n=22; **10µM NKH**, n=21; **30µM NKH**, n=21). Each group combines the data from 3 cover slips. ANOVA with Tukey multiple comparison to compare the means of the groups to each other. **C.** $[LL]_{out}$ increases in a conc-dependent manner following 15min incubation of NKH. Each group has n=6. Kruskal-Wallis test with post-hoc multiple comparisons to compare the means of the groups to the control. Significance asterisks are defined at: ** = p≤0.01, **** = p≤0.0001.

The activation of AC by NKH increased LL levels in astrocytes in a concentration dependent manner up to 3μM *(fig11B)* . Interestingly, from 10μM NKH477, the intracellular LL concentration was not different from control *(fig11B).*

This raises the possibility that NKH at concentrations from 10 μM caused increased LL release. In order to test this, we measured the levels of LL in conditioned media after 15mins incubation with NKH. There was an upward trend in LL release with 1μM to 3μM NKH, and a significant increase at 10μM NKH *(fig11C)*. These results support the idea that >3μM NKH may stimulate LL release. This suggests the boundary in which concentration of LL produced exceeds the concentration necessary for release lies between 3μM NKH and 10μM NKH. Surprisingly, 30μM NKH resulted in a decrease in LL production which was reflected by no measurable change in release. The mechanism behind this complex concentration dependence is yet to be uncovered.

3.2.3. Gi/o-signalling downregulates AC-stimulated LL production

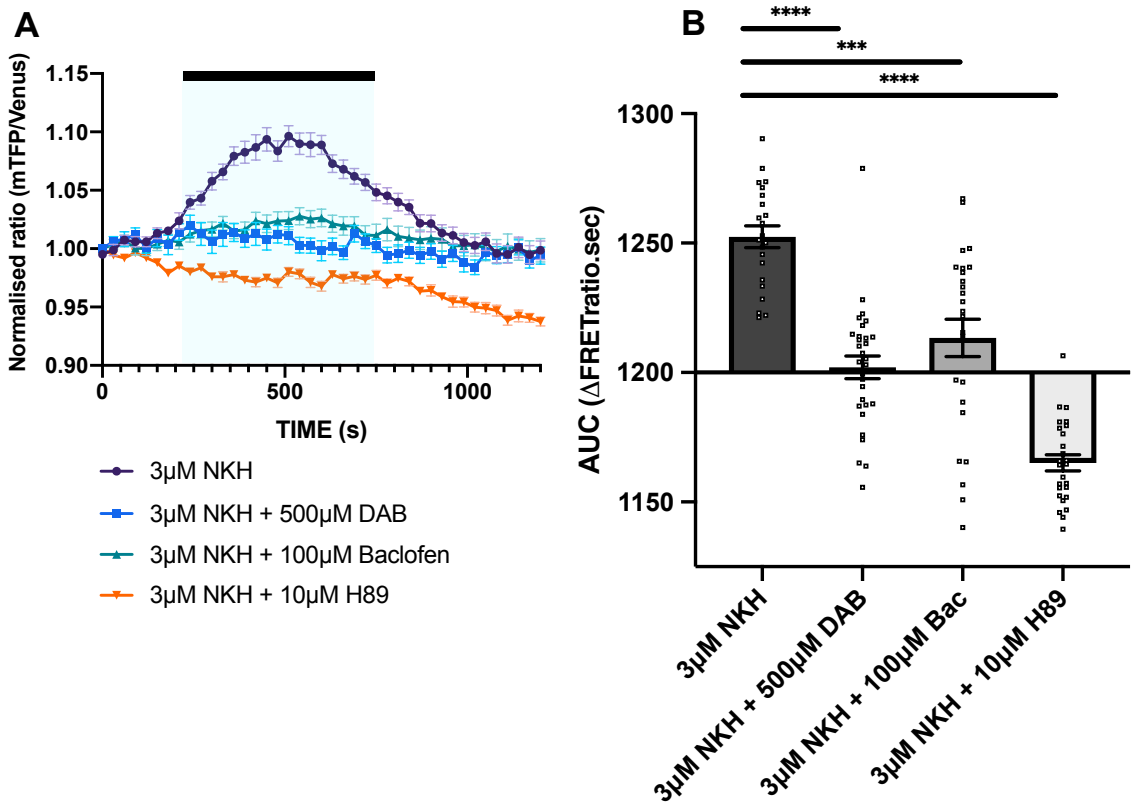

Fig12. Baclofen significantly decreases LL production when AC is stimulated; DAB and H89 mimic this effect. A. Normalized laconic FRET ratio in response to 3μM NKH (n=22, c/s 3) alone or in combination with 100μM Baclofen (n=25, c/s 3), 500μM DAB (n=30, c/s 3) or H89 (n=26, c/s 3). Application between 210-750sec. **B.** Calculated AUC over 1200sec in response to drug application. Each group is the data from 3c/s. Welch ANOVA with Dunnett's T3 multiple comparison to compare the means of the groups to 3μM NKH. Significance asterisks are defined at: *** = p≤0.001, **** = p≤0.0001.

In order to determine the intracellular mediators which facilitate LL production, we measured intracellular LL stimulated with 3μM NKH, in combination with the $GABA_B$ receptor agonist baclofen or the PKA inhibitor H89, or following pre-treatment with the glycogenolysis inhibitor DAB (for 90 mins). 100μM Baclofen inhibited the $[LL]_i$ increase in response to to 3μM NKH *(Fig12B)*. This suggests that the $G_s/G_{i/o}$-coupled GPCR axis impacts on AC's effect on LL production. Similarly, pre-incubation with 500μM DAB completely abolished the $[LL]_i$ increase in response to 3μM NKH. 3μM NKH with 10μM H89 resulted in further decrease in $[LL]_i$ when compared to 3μM NKH *(Fig12B)*. This suggest that both glycogenolysis and PKA activity play a role in AC-stimulated LL production.

3.2.4. Inhibition of $G_{i/o}$ protein signalling with PTX does not block baclofen effects on AC-stimulated LL production

We pre-incubated astrocyte cultures PTX in order to assess the effect of $G_{i/o}$ signalling on stimulated LL production. Surprisingly, pre-incubation with 100ng/µl PTX appeared to potentiate the effect of 100µM Baclofen on the LL levels of astrocytes pre-stimulated with 3µM NKH *(fig13B)*. Conventional understanding would suggest that disabling $G_{i/o}$ signalling should nullify the effect of baclofen. Since this result was opposite to what we were expecting, we went on to explore whether disabling $G_{i/o}$ signalling results in an increase in LL release.

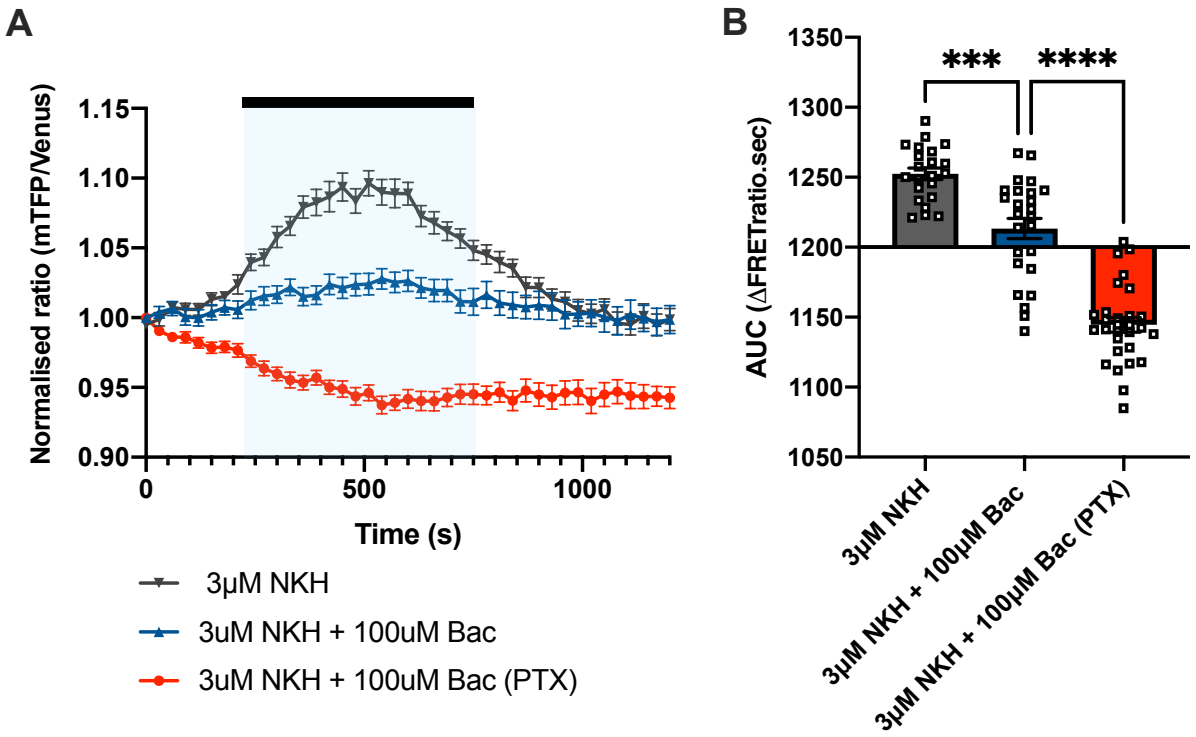

Fig13. PTX pre-incubation does not restore AC-stimulated LL production with baclofen in astrocytes. A. normalized laconic FRET ratio in response to 3µM NKH (n=22, c/s 3), 3µM NKH + 100µM Bac (n=30, c/s 3) and 3µM NKH + 100µM Bac with 24hr pre-incubation of 100ng/µl PTX. Application was 210-750secs. **B.** Calculated AUC over 1200sec in response to drug application. Kruskal Wallis with post-hoc multiple comparisons to compare the means of the groups to each other. Significance asterisks are defined at: *** = $p \leq 0.001$, **** = $p \leq 0.0001$.

3.2.5. Inhibiting $G_{i/o}$ signalling with PTX stimulates LL release in response to baclofen

Pre-treatment of astrocytes with PTX affected the release of LL. 10μM Baclofen showed no statistical difference from control in LL release over a 15min period *(fig14)*. Application of 10μM Baclofen in PTX-treated astrocytes resulted in a statistically significant increase from control *(fig14).* 100ng/ml PTX incubation alone showed a trend towards an increase in LL release but did not show significance in the when compared to the control (*fig14).*

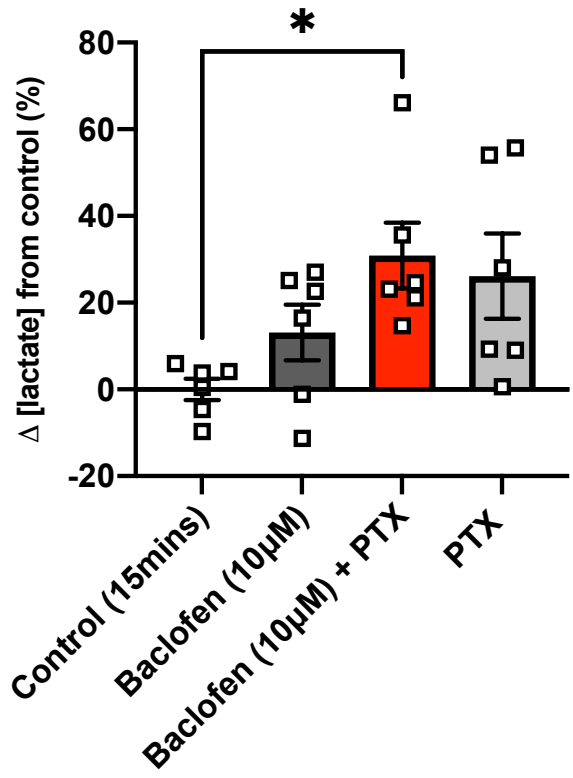

Fig14. PTX pre-incubation increases LL release in response to baclofen. [$LL]_{out}$ following 15min incubation of Baclofen. Each group has n=6. Kruskal-Wallis test with post-hoc multiple comparisons to compare the means of the groups to each other. Significance asterisks are defined at: * = p≤0.05.

4. Discussion

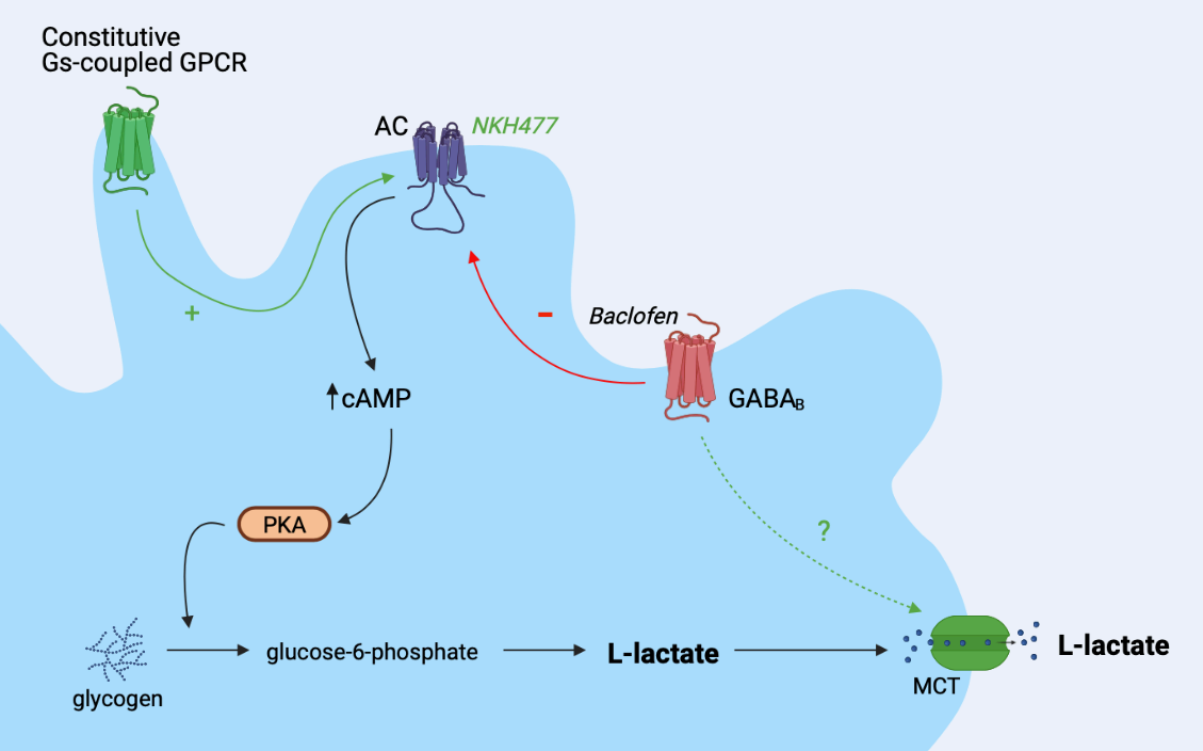

Fig15. GABA$_B$ signalling inhibits basal and AC-stimulated LL production and release via G$_{i/o}$-protein inhibition of AC. Increase in cAMP activates PKA which phosphorylates enzymes which undertake glycogenolysis. LL is then produced which, when the concentration gradient permits, is released via MCTs. An unknown mechanism of GABA$_B$ activation independently of G$_{i/o}$-signalling results in LL release.

4.1. Technical limitations of measuring LL mobilisation

It is not straightforward to measure LL mobilisation, i.e. the combination of LL production and release, as both processes are regulated dynamically and, apparently to some extent, independently. With our approaches that allow us to either measure intra- or extracellular LL changes, we miss part of the information in a highly dynamic system.

An example are our data using the Laconic sensor which suggested that 100µM baclofen had no effect on LL production. Only once we blocked the movement of LL out of the astrocytes were we able to observe the effect of the G$_{i/o}$-signalling. This highlights how, when measuring [LL]$_i$, one is competing with LL release. As such, any change in [LL]$_i$ can be due to or masked by the simultaneous import or release of LL.

An additional confounding factor is the difference in resolution between our approaches to intra- and extracellular LL measurement. With the fluorometric assay which we used for measuring LL in conditioned media, we were limited by the fact that the cultured layer of astrocytes is releasing into a large volume of media. This means that small changes in $[LL]_{out}$ over short observation periods are possibly below the resolution of this approach. This form of assay, therefore, lends itself to sampling over extended time periods, such as the 6-hour incubation shown in Fig3C. However, when using GPCR agonists, one must account for receptor desensitisation and a 6-hour incubation may not be relevant. Therefore, new extracellular tools to measure LL release could help alleviate these drawbacks.

These factors must be taken into consideration when interpreting data on LL mobilisation.

4.2. AC activity helps maintain basal intracellular LL pool in astrocytes

Both $G_{i/o}$-signalling and GP inhibition resulted in a decrease in basal LL mobilisation *(fig7,8,9)*. It, therefore, seems plausible that constitutive AC activity drives LL mobilisation derived from glycogenolysis.

In fact, there are examples of tonic AC activity driven by constitutive G_s-coupled GPCRs which effect LL mobilisation. Recently, β1-adrenoceptor antagonism via CGP-20712 has been shown to inhibit basal release of LL following glucose-starvation, a process attributed to glycogen turnover (Jaing et al., 2020). In keeping with Jaing et al., our results indicate that a source of basal LL production and release is glycogen turnover. However, a question which should be addressed in future experiments is whether the effect of both $G_{i/o}$-signalling and glycogenolysis inhibition summates. If both applied simultaneously result in an additive decrease in LL mobilisation under basal conditions, this theory could be more confidently proposed. Constitutive GPCR mediated glycogenolysis provides interesting avenues for altering LL mobilisation, such as inverse agonists.

Intracellularly, there is a discrepancy between the level of reduction in $[LL]_i$ following the blockade of glycogenolysis compared to AC inhibition (*fig7, fig9B*). Application of DAB inhibited AR-C meditated LL build-up by ~25%. Therefore, a significant proportion of LL produced at basal conditions must be derived independent of glycogen, presumably through the aerobic glycolysis of glucose. In contrast , Baclofen application (even at 10μM) resulted in a decrease in $[LL]_i$ of ~85%. This could be interpreted as an increase in release but this was not observable in our release assay (*fig8).* Therefore, this would suggest that the effect of Baclofen is not confined to inhibition of glycogenolysis.

Interestingly, astrocytes incubated in no glucose media for 6hrs *(fig9C)* showed a large variation in $[LL]_{out}$ even when glycogenolysis was blocked by DAB. Therefore, astrocytes are clearly able to produce LL by a mechanism independent of glycogenolysis or glycolysis.

The effect $GABA_B$ signalling has on alternate LL production routes remains unclear. There is evidence that inhibition of PKA-mediated phosphorylation of mitochondrial complex proteins by the $G_{i/o}$-coupled CB1 receptor results in a decrease in $[LL]_i$ (Jimenez-Blasco et al., 2020). Similarly, it is possible that reduction in cAMP in astrocytes has an effect on mitochondrial activity. However, the time course of agonist application was comparatively longer than our application (24hr). Despite this, this does suggest that AC-activation, and PKA activity, has a role in LL production beyond glycogenolysis.

4.3. AC activity stimulates LL mobilisation in astrocytes

We found an unexpected concentration dependent effect of NKH on LL production and release *(fig11)*. While these results necessitate further investigation, other groups have reported that cAMP can regulate LL mobilisation in astrocytes. Various studies have shown activation of G_s-coupled GPCRs stimulates glycogenolysis (Sorg and Magistretti, 1991; Subbarao and Hertz, 1990). Further, in line with our evidence, Choi et al. showed that sAC, a variant of AC not directly linked to GPCR activity, resulted in glycogen breakdown and LL release (Choi et al., 2012).

Interestingly, it was recently reported by Horvat et al that stimulation of both the α1 and β adrenoceptors was required to induce a significant increase in $[LL]_i$ (Horvat et al., 2021). The authors emphasised the importance of Ca^{2+}-signalling in this example by reporting that the cAMP-signalling induced by β-adrenoceptor (G_s-coupled) signalling alone did not yield a significant increase in $[LL]_i$. Our results show that raising cAMP levels by direct AC stimulation can significantly increase LL mobilisation. However, without assessing or directly stimulating intracellular Ca^{2+} increase simultaneously, we cannot discount that Ca^{2+} signalling may have played a role in LL production in our experiments.

Following NKH application, the concentration range in which there was an observed difference in $[LL]_i$ was small (3μM-10μM NKH). By comparing dynamics of $[LL]_i$ with those of $[LL]_{out}$, we were able to determine that the concentration for NKH application in which the $[LL]_i > [LL]_{out}$ lies between 3μM-10μM. The experimental HBS solution does not contain any LL, rendering the $[LL]_{out}$ 0mM in our imaging studies. Therefore, theoretically, all LL produced should be released into the bath. However, this could depend on the MCTs which are expressed in the astrocyte cultures we used. Astrocytes are generally assumed to express MCT1/4 (Pellerin et al., 2005). MCT1 is reported to have a higher

affinity for LL when compared to MCT4 (Juel and Halestrap, 1999). AR-C, an MCT1 blocker, resulted in $[LL]_i$ accumulation in our astrocytes. As such, one could assume that the $[LL]_i$ produced between 3μM-10μM NKH is in the K_D range of MCT1, 5-10mM (Juel and Halestrap, 1999). However, this would have to be confirmed by observing whether the LL released in response to 10μM NKH is inhibited by AR-C application.

It is also of interest that 30μM NKH (which would result in high levels of cAMP) inhibits both LL production and release. Astrocytic cAMP has been implicated in regulation of connexin hemichannels, an alternative release route for LL, and also in K^+ buffering and glutamate uptake (Zhou et al., 2019). High levels of cAMP may therefore disrupt many processes which could have an effect on LL mobilisation.

We report that LL mobilisation via cAMP signalling is dependent on glycogenolysis. Recently, via measuring LL output and glycogen accumulation, it has been suggested that the effect of the G_s-coupled GPCR β1 adrenoceptor on LL release is independent of glycogen turnover (Jiang et al., 2020). If assumed that the LL release caused by β1 adrenoceptor is mediated by an increase in AC activity, this interpretation is contrary to our observation. Application of DAB inhibits GP (Fosgerau et al., 2000) and in our experiments *(fig12)*, completely diminished AC-stimulated LL production. This is similar to the observations of Fink et al that DAB application completely inhibits NA-induced $[LL]_i$ increase (Fink et al., 2021).

PKA functioning is also essential for AC-stimulated LL production. Not only did application of H89 abolish the response of AC-stimulated LL increase, it also resulted in a decrease in $[LL]_i$ beyond baseline levels *(fig12).* This decrease was not observed with DAB application. Therefore, this suggest PKA must have effects on LL production which are independent of glycogen degradation.

4.4. $GABA_B$ signalling inhibits AC-stimulated LL production in astrocytes

$GABA_B$ activation has been reported to induce Ca^{2+} oscillations in astrocytes (Mariotti et al., 2016). Ca^{2+} has been implicated in stimulating glycogenolysis, specifically via $GABA_B$ signalling (Xu et al., 2014). With more time afforded, clarification about whether baclofen stimulates Ca^{2+} signalling in our cultures with a calcium sensor is essential. However, we report no stimulatory effect of $GABA_B$ activation on LL mobilisation. Baclofen application up to 100μM showed no increase in production or release. This would suggest intracellular Ca^{2+} does not regulate LL mobilisation. Instead, our data suggests that stimulated LL mobilisation is regulated by the competitive action of G_s-coupled and $G_{i/o}$-coupled GPCRs and their effect on AC activity. It would be important to try Baclofen in

combination with DAB in order to confirm that this inhibition of LL mobilisation is directly via glycogen turnover.

One such discrepancy may arise from the used of cultured astrocytes. As shown in (Mariotti et al., 2018), the stimulation Ca^{2+} oscillations in vivo is not homologous throughout all cortical areas. In the somatosensory cortex, for example, Ca^{2+} oscillations were not observed without co-activation of the somatostatin receptor 4 (SST4R) (Mariotti et al., 2018). It is therefore possible that our astrocyte cultures lacked the necessary protein expression to cause Ca^{2+} oscillations. Further, there is evidence that $GABA_B$ -mediated Ca^{2+} signals in cultured astrocytes are dependent on pre-activation of P2YRs (Terunuma et al., 2015).

We report that inhibition of $G_{i/o}$ signalling by PTX does not restore AC-stimulated LL mobilisation following $GABA_B$ activation. In fact, we observed the opposite in that we saw a decrease in $[LL]_i$. Without further data, there could be multiple explanations for this. Interestingly, G_q-protein knockdown in neurones abolished $GABA_B$ -mediated Ca^{2+} signalling (Karls and Mynlieff, 2015). The mechanism behind $GABA_B$-mediated Ca^{2+} signalling in astrocytes is unclear. However, if $GABA_B$ receptors in astrocytes were able to couple to G_q similarly to neurones, inhibiting coupling of the $G_{i/o}$-protein may enhance coupling of the G_q-protein. This is complicated by the fact that PTX treatment inhibits Ca^{2+} in response to baclofen (Mariotti et al., 2016). However, although not statistically validated in Mariotti et al., PTX treatment does seem to increase the Ca^{2+} activity of astrocytes. Therefore, it is clear that the blunt inhibition of all undefined $G_{i/o}$-coupled GPCRs has wide reaching effects on the cell and, in turn, LL mobilisation. Specific protein knockdown of G_q-proteins, G_i-proteins and AC are needed in order to understand the mechanism behind this decrease in $[LL]_i$.

Despite the decrease in $[LL]_i$ following AC-activation and $GABA_B$ activation in the presence of PTX, the data we present on LL release following PTX incubation hints that PTX results in an increase in $[LL]_{out}$. This would suggest there is a discrepancy between LL production and release in this scenario. Therefore, in order to explore the possibility of a novel release mechanism, it would be interesting to try MCT blockers in combination with baclofen in the presence of PTX for measurement of LL release. It will also be important to confirm the effect of AC-stimulated LL mobilisation in the presence of PTX on release - work we were unable to complete due to time restrictions.

4.5. Conclusions and future perspectives

In our work, we confirm the inhibitory effect of $GABA_B$ signalling on basal LL production. We can also confirm that glycogen utilization helps facilitate LL mobilisation under basal conditions. We are also able to confirm that AC-mediated cAMP signalling can facilitate LL mobilisation – an effect that was

inhibited by blocking glycogen utilisation and PKA activity. In our cultures, $GABA_B$ signalling inhibits stimulated LL mobilisation. Clearly, our study raises a number of questions which need more work to answer. Essential would be to identify whether Ca^{2+} signals are evoked by $GABA_B$ activation in our astrocytic culture. Also essential would be to clarify whether the addition of both Baclofen and DAB summates the inhibition of both basal and AC-stimulated LL mobilisation. With this data, one could identify further whether the effect of $GABA_B$ signalling is wholly dependent on glycogenolysis in each scenario. Significant gaps in our data need to be addressed in order to make conducive conclusions. Given the physiological implications of astrocytic $GABA_B$ signalling and astrocytic LL release, work on this topic may provide greater insight into astrocytic modulation of neuronal functioning.

5. COVID-19 Statement

Due to the closure of laboratories during the COVID-19 pandemic, experimental work was disrupted and overall limited, resulting in a reduction of some of the datasets in this study.

6. Acknowledgements

I would like to give special thanks to Anja Teschemacher for her all-encompassing support and guidance over the course of this project. I would also like to thank Sergey Kasparov, Barbara Vaccari Cardoso, Lesley Arberry and Iliana Barrera for all their help in the laboratory.

7. References

- Allaman, I., Fiumelli, H., Magistretti, P.J., and Martin, J.L. (2011). Fluoxetine regulates the expression of neurotrophic/growth factors and glucose metabolism in astrocytes. Psychopharmacology (Berl) *216*, 75-84.
- Allen, N.J. (2014). Astrocyte regulation of synaptic behavior. Annu Rev Cell Dev Biol *30*, 439-463.
- Barros, L.F. (2013). Metabolic signaling by lactate in the brain. Trends in Neurosciences *36*, 396-404.
- Bazargani, N., and Attwell, D. (2016). Astrocyte calcium signaling: the third wave. Nat Neurosci *19*, 182-189.
- Bett, A.J., Haddara, W., Prevec, L., and Graham, F.L. (1994). An efficient and flexible system for construction of adenovirus vectors with insertions or deletions in early regions 1 and 3. Proceedings of the National Academy of Sciences of the United States of America *91*, 8802-8806.
- Cai, T.Q., Ren, N., Jin, L., Cheng, K., Kash, S., Chen, R., Wright, S.D., Taggart, A.K., and Waters, M.G. (2008). Role of GPR81 in lactate-mediated reduction of adipose lipolysis. Biochem Biophys Res Commun *377*, 987-991.
- Cataldo, A.M., and Broadwell, R.D. (1986). Cytochemical identification of cerebral glycogen and glucose-6-phosphatase activity under normal and experimental conditions. II. Choroid plexus and ependymal epithelia, endothelia and pericytes. J Neurocytol *15*, 511-524.
- Choi, Hyun B., Gordon, Grant R.J., Zhou, N., Tai, C., Rungta, Ravi L., Martinez, J., Milner, Teresa A., Ryu, Jae K., McLarnon, James G., Tresguerres, M., et al. (2012). Metabolic

Communication between Astrocytes and Neurons via Bicarbonate-Responsive Soluble Adenylyl Cyclase. Neuron *75*, 1094-1104.

- Chuquet, J., Quilichini, P., Nimchinsky, E.A., and Buzsaki, G. (2010). Predominant enhancement of glucose uptake in astrocytes versus neurons during activation of the somatosensory cortex. J Neurosci *30*, 15298-15303.
- Colombo, E., and Farina, C. (2016). Astrocytes: Key Regulators of Neuroinflammation. Trends Immunol *37*, 608-620.
- Diaz-Garcia, C.M., Mongeon, R., Lahmann, C., Koveal, D., Zucker, H., and Yellen, G. (2017). Neuronal Stimulation Triggers Neuronal Glycolysis and Not Lactate Uptake. Cell Metab *26*, 361-374 e364.
- Dienel, G.A. (2017). Lack of appropriate stoichiometry: Strong evidence against an energetically important astrocyte-neuron lactate shuttle in brain. J Neurosci Res *95*, 2103-2125.
- Fink, K., Velebit, J., Vardjan, N., Zorec, R., and Kreft, M. (2021). Noradrenaline-induced l-lactate production requires d-glucose entry and transit through the glycogen shunt in single-cultured rat astrocytes. J Neurosci Res *99*, 1084-1098.
- Fosgerau, K., Westergaard, N., Quistorff, B., Grunnet, N., Kristiansen, M., and Lundgren, K. (2000). Kinetic and functional characterization of 1,4-dideoxy-1, 4-imino-d-arabinitol: a potent inhibitor of glycogen phosphorylase with anti-hyperglyceamic effect in ob/ob mice. Arch Biochem Biophys *380*, 274-284.
- Gandhi, G.K., Cruz, N.F., Ball, K.K., and Dienel, G.A. (2009). Astrocytes are poised for lactate trafficking and release from activated brain and for supply of glucose to neurons. J Neurochem *111*, 522-536.
- Gao, V., Suzuki, A., Magistretti, P.J., Lengacher, S., Pollonini, G., Steinman, M.Q., and Alberini, C.M. (2016). Astrocytic beta2-adrenergic receptors mediate hippocampal long-term memory consolidation. Proc Natl Acad Sci U S A *113*, 8526-8531.
- Graham, F.L., and Prevec, L. (1995). Methods for construction of adenovirus vectors. Molecular Biotechnology *3*, 207-220.
- Halim, N.D., McFate, T., Mohyeldin, A., Okagaki, P., Korotchkina, L.G., Patel, M.S., Jeoung, N.H., Harris, R.A., Schell, M.J., and Verma, A. (2010). Phosphorylation status of pyruvate dehydrogenase distinguishes metabolic phenotypes of cultured rat brain astrocytes and neurons. Glia *58*, 1168-1176.
- Hertz, L., Peng, L., and Dienel, G.A. (2007). Energy metabolism in astrocytes: high rate of oxidative metabolism and spatiotemporal dependence on glycolysis/glycogenolysis. J Cereb Blood Flow Metab *27*, 219-249.
- Horvat, A., Muhic, M., Smolic, T., Begic, E., Zorec, R., Kreft, M., and Vardjan, N. (2021). Ca(2+) as the prime trigger of aerobic glycolysis in astrocytes. Cell Calcium *95*, 102368.
- Jiang, X., Challiss, J., and Glynn, P. (2020). beta1-adrenoceptor-stimulated lactate production in cultured astrocytes is predominantly glycogen-independent. Biochem Pharmacol *177*, 114035.
- Jimenez-Blasco, D., Busquets-Garcia, A., Hebert-Chatelain, E., Serrat, R., Vicente-Gutierrez, C., Ioannidou, C., Gomez-Sotres, P., Lopez-Fabuel, I., Resch-Beusher, M., Resel, E., et al. (2020). Glucose metabolism links astroglial mitochondria to cannabinoid effects. Nature *583*, 603-608.

- Jourdain, P., Rothenfusser, K., Ben-Adiba, C., Allaman, I., Marquet, P., and Magistretti, P.J. (2018). Dual action of L-Lactate on the activity of NR2B-containing NMDA receptors: from potentiation to neuroprotection. Sci Rep *8*, 13472.
- Juel, C., and Halestrap, A.P. (1999). Lactate transport in skeletal muscle — role and regulation of the monocarboxylate transporter. The Journal of Physiology *517*, 633-642.
- Karls, A., and Mynlieff, M. (2015). GABA(B) receptors couple to Galphaq to mediate increases in voltage-dependent calcium current during development. J Neurochem *135*, 88-100.
- Karnib, N., El-Ghandour, R., El Hayek, L., Nasrallah, P., Khalifeh, M., Barmo, N., Jabre, V., Ibrahim, P., Bilen, M., Stephan, J.S., et al. (2019). Lactate is an antidepressant that mediates resilience to stress by modulating the hippocampal levels and activity of histone deacetylases. Neuropsychopharmacology *44*, 1152-1162.
- Kirischuk, S., Heja, L., Kardos, J., and Billups, B. (2016). Astrocyte sodium signaling and the regulation of neurotransmission. Glia *64*, 1655-1666.
- Kofuji, P., and Araque, A. (2021). G-Protein-Coupled Receptors in Astrocyte-Neuron Communication. Neuroscience *456*, 71-84.
- Lauritzen, K.H., Morland, C., Puchades, M., Holm-Hansen, S., Hagelin, E.M., Lauritzen, F., Attramadal, H., Storm-Mathisen, J., Gjedde, A., and Bergersen, L.H. (2014). Lactate receptor sites link neurotransmission, neurovascular coupling, and brain energy metabolism. Cereb Cortex *24*, 2784-2795.
- Machler, P., Wyss, M.T., Elsayed, M., Stobart, J., Gutierrez, R., von Faber-Castell, A., Kaelin, V., Zuend, M., San Martin, A., Romero-Gomez, I., et al. (2016). In Vivo Evidence for a Lactate Gradient from Astrocytes to Neurons. Cell Metab *23*, 94-102.
- Maher, F., Vannucci, S.J., and Simpson, I.A. (1994). Glucose transporter proteins in brain. The FASEB Journal *8*, 1003-1011.
- Mariotti, L., Losi, G., Lia, A., Melone, M., Chiavegato, A., Gómez-Gonzalo, M., Sessolo, M., Bovetti, S., Forli, A., Zonta, M., et al. (2018). Interneuron-specific signaling evokes distinctive somatostatin-mediated responses in adult cortical astrocytes. Nat Commun *9*, 82.
- Mariotti, L., Losi, G., Sessolo, M., Marcon, I., and Carmignoto, G. (2016). The inhibitory neurotransmitter GABA evokes long-lasting Ca(2+) oscillations in cortical astrocytes. Glia *64*, 363-373.
- Mederos, S., Sanchez-Puelles, C., Esparza, J., Valero, M., Ponomarenko, A., and Perea, G. (2021). GABAergic signaling to astrocytes in the prefrontal cortex sustains goal-directed behaviors. Nat Neurosci *24*, 82-92.
- Mosienko, V., Rasooli-Nejad, S., Kishi, K., De Both, M., Jane, D., Huentelman, M., Kasparov, S., and Teschemacher, A. (2018). Putative Receptors Underpinning l-Lactate Signalling in Locus Coeruleus. Neuroglia *1*, 365-380.
- Mosienko, V., Teschemacher, A.G., and Kasparov, S. (2015). Is L-lactate a novel signaling molecule in the brain? J Cereb Blood Flow Metab *35*, 1069-1075.
- Nadeau, O.W., Fontes, J.D., and Carlson, G.M. (2018). The regulation of glycogenolysis in the brain. J Biol Chem *293*, 7099-7107.
- Navarrete, M., and Araque, A. (2010). Endocannabinoids Potentiate Synaptic Transmission through Stimulation of Astrocytes. Neuron *68*, 113-126.
- Oe, Y., Wang, X., Patriarchi, T., Konno, A., Ozawa, K., Yahagi, K., Hirai, H., Tian, L., McHugh, T.J., and Hirase, H. (2020). Distinct temporal integration of noradrenaline signaling by astrocytic second messengers during vigilance. Nat Commun *11*, 471.

- Pankratov, Y., and Lalo, U. (2015). Role for astroglial α1-adrenoreceptors in gliotransmission and control of synaptic plasticity in the neocortex. Front Cell Neurosci *9*, 230-230.
- Pellerin, L., Halestrap, A.P., and Pierre, K. (2005). Cellular and subcellular distribution of monocarboxylate transporters in cultured brain cells and in the adult brain. Journal of Neuroscience Research *79*, 55-64.
- Pellerin, L., and Magistretti, P.J. (1994). Glutamate uptake into astrocytes stimulates aerobic glycolysis: a mechanism coupling neuronal activity to glucose utilization. Proceedings of the National Academy of Sciences *91*, 10625-10629.
- Pellerin, L., and Magistretti, P.J. (2012). Sweet sixteen for ANLS. J Cereb Blood Flow Metab *32*, 1152-1166.
- Perea, G., Gomez, R., Mederos, S., Covelo, A., Ballesteros, J.J., Schlosser, L., Hernandez-Vivanco, A., Martin-Fernandez, M., Quintana, R., Rayan, A., et al. (2016). Activity-dependent switch of GABAergic inhibition into glutamatergic excitation in astrocyte-neuron networks. Elife *5*.
- Pfeiffer-Guglielmi, B., Fleckenstein, B., Jung, G., and Hamprecht, B. (2003). Immunocytochemical localization of glycogen phosphorylase isozymes in rat nervous tissues by using isozyme-specific antibodies. J Neurochem *85*, 73-81.
- Pierre, K., and Pellerin, L. (2005). Monocarboxylate transporters in the central nervous system: distribution, regulation and function. J Neurochem *94*, 1-14.
- Rasooli-Nejad, S., Palygin, O., Lalo, U., and Pankratov, Y. (2014). Cannabinoid receptors contribute to astroglial Ca^{2+}-signalling and control of synaptic plasticity in the neocortex. Philos Trans R Soc Lond B Biol Sci *369*, 20140077-20140077.
- San Martin, A., Ceballo, S., Ruminot, I., Lerchundi, R., Frommer, W.B., and Barros, L.F. (2013). A genetically encoded FRET lactate sensor and its use to detect the Warburg effect in single cancer cells. PLoS One *8*, e57712.
- Sorg, O., and Magistretti, P.J. (1991). Characterization of the glycogenolysis elicited by vasoactive intestinal peptide, noradrenaline and adenosine in primary cultures of mouse cerebral cortical astrocytes. Brain Res *563*, 227-233.
- Sorg, O., Pellerin, L., Stolz, M., Beggah, S., and Magistretti, P.J. (1995). Adenosine triphosphate and arachidonic acid stimulate glycogenolysis in primary cultures of mouse cerebral cortical astrocytes. Neuroscience Letters *188*, 109-112.
- Sotelo-Hitschfeld, T., Niemeyer, M.I., Machler, P., Ruminot, I., Lerchundi, R., Wyss, M.T., Stobart, J., Fernandez-Moncada, I., Valdebenito, R., Garrido-Gerter, P., et al. (2015). Channel-mediated lactate release by K(+)-stimulated astrocytes. J Neurosci *35*, 4168-4178.
- Subbarao, K.V., and Hertz, L. (1990). Effect of adrenergic agonists on glycogenolysis in primary cultures of astrocytes. Brain Res *536*, 220-226.
- Supplie, L.M., Duking, T., Campbell, G., Diaz, F., Moraes, C.T., Gotz, M., Hamprecht, B., Boretius, S., Mahad, D., and Nave, K.A. (2017). Respiration-Deficient Astrocytes Survive As Glycolytic Cells In Vivo. J Neurosci *37*, 4231-4242.
- Suzuki, A., Stern, S.A., Bozdagi, O., Huntley, G.W., Walker, R.H., Magistretti, P.J., and Alberini, C.M. (2011). Astrocyte-neuron lactate transport is required for long-term memory formation. Cell *144*, 810-823.
- Tadi, M., Allaman, I., Lengacher, S., Grenningloh, G., and Magistretti, P.J. (2015). Learning-Induced Gene Expression in the Hippocampus Reveals a Role of Neuron -Astrocyte Metabolic Coupling in Long Term Memory. PLoS One *10*, e0141568.

- Tang, F., Lane, S., Korsak, A., Paton, J.F., Gourine, A.V., Kasparov, S., and Teschemacher, A.G. (2014). Lactate-mediated glia-neuronal signalling in the mammalian brain. Nat Commun *5*, 3284.
- Terunuma, M., Haydon, P.G., Pangalos, M.N., and Moss, S.J. (2015). Purinergic receptor activation facilitates astrocytic GABAB receptor calcium signalling. Neuropharmacology *88*, 74-81.
- Vaccari Cardoso, B., Shevelkin, A.V., Terrillion, C., Mychko, O., Mosienko, V., Kasparov, S., Pletnikov, M.V., and Teschemacher, A.G. (2021). Reducing l-lactate release from hippocampal astrocytes by intracellular oxidation increases novelty induced activity in mice. Glia *69*, 1241-1250.
- Vardjan, N., Chowdhury, H.H., Horvat, A., Velebit, J., Malnar, M., Muhič, M., Kreft, M., Krivec, Š., Bobnar, S.T., Miš, K., et al. (2018). Enhancement of Astroglial Aerobic Glycolysis by Extracellular Lactate-Mediated Increase in cAMP. Front Mol Neurosci *11*, 148.
- Verkhratsky, A., Matteoli, M., Parpura, V., Mothet, J.-P., and Zorec, R. (2016). Astrocytes as secretory cells of the central nervous system: idiosyncrasies of vesicular secretion. The EMBO Journal *35*, 239-257.
- Xu, J., Song, D., Bai, Q., Cai, L., Hertz, L., and Peng, L. (2014). Basic mechanism leading to stimulation of glycogenolysis by isoproterenol, EGF, elevated extracellular K+ concentrations, or GABA. Neurochem Res *39*, 661-667.
- Yang, J., Ruchti, E., Petit, J.M., Jourdain, P., Grenningloh, G., Allaman, I., and Magistretti, P.J. (2014). Lactate promotes plasticity gene expression by potentiating NMDA signaling in neurons. Proc Natl Acad Sci U S A *111*, 12228-12233.
- Zhang, X., Peng, L., Chen, Y., and Hertz, L. (1993). Stimulation of glycogenolysis in astrocytes by fluoxetine, an antidepressant acting like 5-HT. Neuroreport *4*, 1235-1238.
- Zhang, Y., Chen, K., Sloan, S.A., Bennett, M.L., Scholze, A.R., O'Keeffe, S., Phatnani, H.P., Guarnieri, P., Caneda, C., Ruderisch, N., et al. (2014). An RNA-sequencing transcriptome and splicing database of glia, neurons, and vascular cells of the cerebral cortex. J Neurosci *34*, 11929-11947.
- Zhou, Z., Ikegaya, Y., and Koyama, R. (2019). The Astrocytic cAMP Pathway in Health and Disease. Int J Mol Sci *20*.
- Zuend, M., Saab, A.S., Wyss, M.T., Ferrari, K.D., Hösli, L., Looser, Z.J., Stobart, J.L., Duran, J., Guinovart, J.J., Barros, L.F., et al. (2020). Arousal-induced cortical activity triggers lactate release from astrocytes. Nature Metabolism *2*, 179-191.